Role of Inter-Cluster and Inter-Ligand Dynamics of $[Ag_{25}(DMBT)_{18}]^-$ Nanoclusters by Multinuclear Magnetic Resonance Spectroscopy.

Giovanni Salassa[a],*,K. R. Krishnadas[a], Marion Pupier,[b] Jasmine Viger-Gravel,[b],* Thomas Bürgi[a],*

[a]*Department of Physical Chemistry, University of Geneva, 30 Quai Ernest-Ansermet, 1211 Geneva 4, Switzerland.*
[b]*Department of Organic Chemistry, University of Geneva, 30 Quai Ernest-Ansermet, 1211 Geneva 4, Switzerland*

Supporting Information

Table of Contents

1. Experimental procedures

Chemicals

Silver nitrate ($AgNO_3$, Merck, 99%), chloro(triphenylphosphine)gold(I) ($AuClPPh_3$, Merck, 99.9+%), sodium borohydride (Fluka, > 96%), tetraoctylammonium bromide (TOABr, Merck, 98%), tetraphenylphosphonium bromide (PPhBr, Merck, 97%), 2,4-dimethylbenzenethiol (Merck, 95%), hexafluorobenzene (Merck, 99%), methanol (VWR, > 99.8%), acetone (Fluka, > 99.5%), methylene chloride (DCM, Merck, > 99.9%), toluene (Merck, 99.9%), PTFE syringe filters (0.2 μm, Carl Roth, Karlsruhe/Germany), recovered cellulose membranes (0.2 μm, Sartorius) and BioBeads S-X1 (BioRad) were used as purchased if not mentioned otherwise. Nanopure water (> 18 MΩ) was used.

Characterization

UV−vis spectra were recorded on a Varian Cary 50 spectrometer. Quartz cuvette of 10 mm path length was used (solvents: methylene chloride and toluene).

Mass spectra were obtained using a QSTAR XL (AB Sciex) with syringe infusion at 10 μl/mL, ESI voltage = 4200 V (negative) with source position V = 7 / H = +3 (laboratory frame). The nebulization gas was N_2 (25 psi), as well as drying gas (10 psi) and curtain gas (20 psi).Declustering and focusing lenses: DP = -110 V, DP2 = -20 V, FP = -250 V. Mass range: m/z 100 – 12'000 (accumulation time = 1s) with external TOF calibration (Agilent), Bin = 1 (automatic signal smoothing). The sample solubilized in dichloromethane.

2. Synthesis of nanocluster compounds

$[Ag_{25}(DMBT)_{18}][TOA]$: $[Ag_{25}(DMBT)_{18}][TOA]$ was synthesized by adopting a reported procedure[1] with slight modifications. 76 mg of $AgNO_3$ were dissolved in about 4 mL of methanol by ultrasonication. The $AgNO_3$ solution, after being transferred into a round bottom flask, was moderately stirred at 0° C (ice bath). 190 μL of pure 2,4-dimethylbenzenethiol were then poured into the $AgNO_3$ solution in one quick addition. Following, 34 mL of DCM were added and the reaction mixture was stirred at about 1400 rpm for about 20 minutes. Then, a freshly prepared solution of TOABr (15 mg, or PPhBr) in 1 mL methanol was added in one shot into the reaction mixture. Then a freshly prepared solution of $NaBH_4$ (30 mg in 1 mL ice cold pure water) was added to the mixture dropwise. The reaction mixture was then stirred at the same speed for about 6 hours in the ice bath. After 6h, the solution was left to age overnight at 4 °C. After this period, the organic fraction of the solution was carefully transferred to a centrifuge tube leaving the insoluble material at the bottom of the flask. The collected organic fraction was then centrifuged at around 10000 rpm for about 10 minutes. After the first centrifugation, the solution is carefully transferred to a round bottom flask and rotary evaporated till the solution becomes a paste-like material; the solution was not dried completely at this stage. Afterward, about 15 mL of methanol is added to the round bottom flask in order to precipitate the clusters from the impurities. Centrifugation at around 10000 rpm for about 10 minutes was used to collect more easily the precipitate, meanwhile the supernatant (methanol solution) was discarded. This washing procedure was repeated 2-3 more times, in order to remove most of the free DMBT ligands and the residues formed from the reducing agents. The collected

precipitate was then dissolved in 15 mL of DCM in the centrifuge tube, the dissolved clusters were centrifuged at around 10000 rpm for about 10 minutes. The solution was carefully transferred to a round bottom flask, leaving any insoluble material at the bottom of the centrifuge tube, and dried using a rotary evaporator. The dried material was then purified with size exclusion chromatography (BioBeads S-X1) using DCM as eluting solvent to obtain pure $[Ag_{25}(DMBT)_{18}][TOA]$ clusters.

$[Ag_{24}Au_1(DMBT)_{18}][TOA]$: $[Ag_{24}Au_1(DMBT)_{18}][TOA]$ was synthesized by the reaction of $[Ag_{25}(DMBT)_{18}][TOA]$ with $AuClPPh_3$ by adopting a reported procedure[2] with slight modifications. 16 mg of $[Ag_{25}(DMBT)_{18}][TOA]$ were dissolved in 5 mL of DCM. 200 μL of $AuClPPh_3$solution (4.2 mg in 500 μL DCM) was then added to it. The reaction mixture was gently shaken with hand for some minutes to allow the mixing of the reagents and then kept unmoved for about 2 hours. The color of the solution changed from dark brown to dark green during this time interval, indicating the formation of $[Ag_{24}Au_1(DMBT)_{18}][TOA]$. Formation of the alloy cluster was confirmed using UV/Vis spectroscopy as well. Then the reaction mixture is passed through a size exclusion chromatographic column using DCM as the eluting solvent. The pure $[Ag_{24}Au_1(DMBT)_{18}][TOA]$ thus obtained was dried using rotary evaporation.

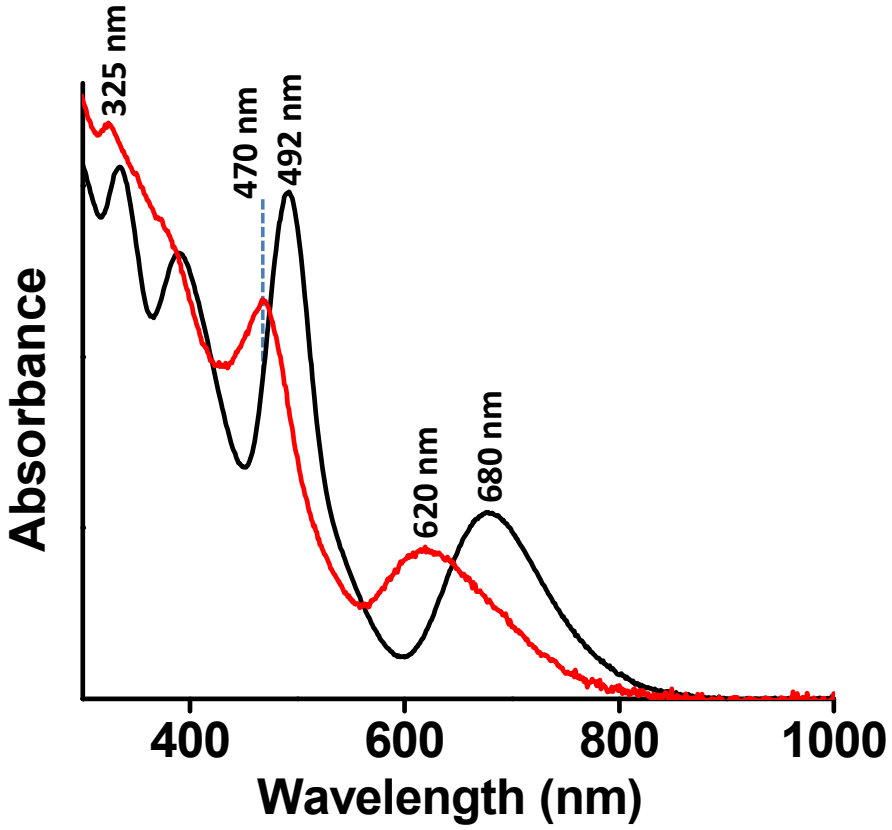

Figure S1. UV/Vis absorption spectra of $[Ag_{25}(DMBT)_{18}][TOA]$ (black trace) and $[Ag_{24}Au_1(DMBT)_{18}][TOA]$ (red trace).

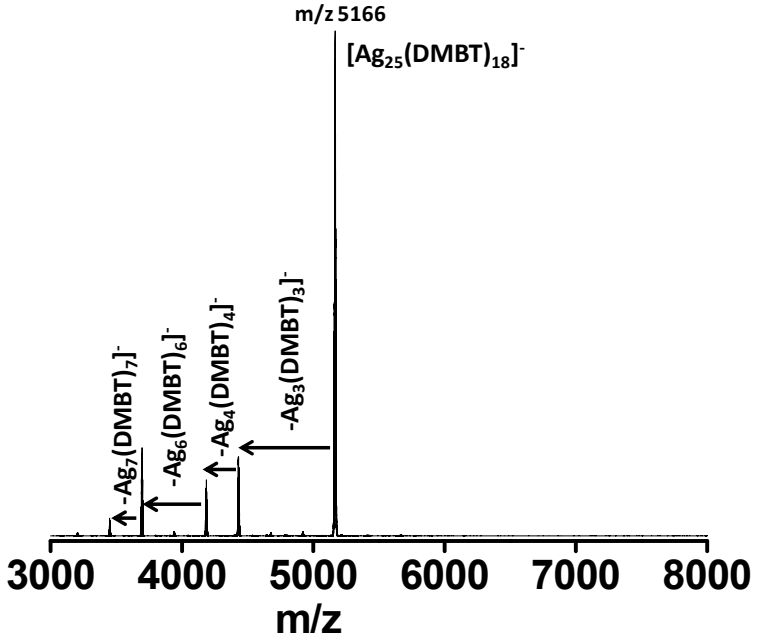

Figure S2. Negative ion mode ESI MS spectrum of $[Ag_{25}(DMBT)_{18}][TOA]$ showing the molecular ion peak of the anion, $[Ag_{25}(DMBT)_{18}]^-$, and its typical fragments formed due to the sequential loss of (Ag-DMBT) units as indicated on top of the arrows.

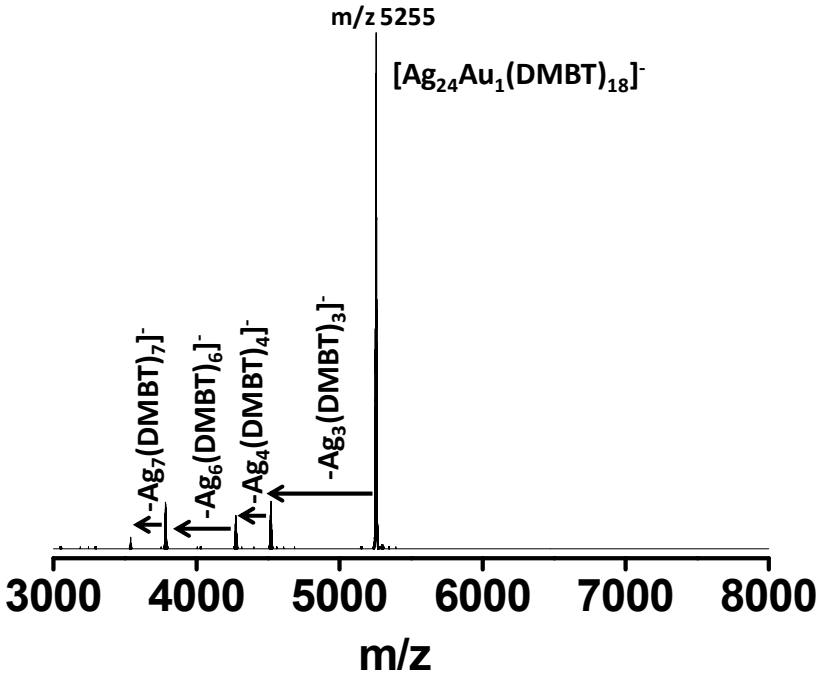

Figure S3. Negative ion mode ESI MS spectrum of $[Ag_{24}Au_1(DMBT)_{18}][TOA]$ showing the molecular ion peak of the anion,$[Ag_{24}Au_1(DMBT)_{18}]^-$, and its typical fragments formed due to the sequential loss of (Ag-DMBT) units as indicated on top of arrows.

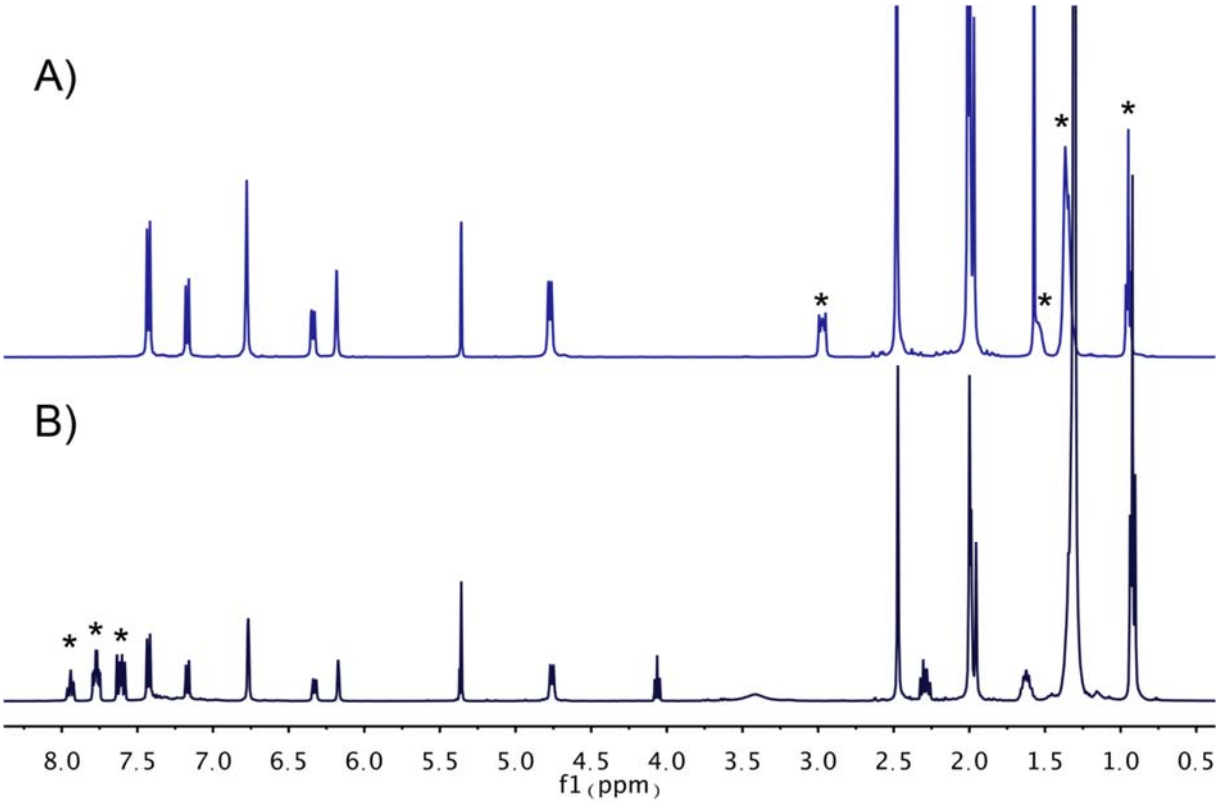

Figure S4: ^{1}H-NMR of $Ag_{25}(DMBT)_{18}$ in DCM-d_2 at 298K in presence of A) tetraoctylammonium (TOA^{+}) and B) tetraphenylphosphonium (PPh^{+}) counterions.

3. Inter-ligand interactions in the reported crystal structure

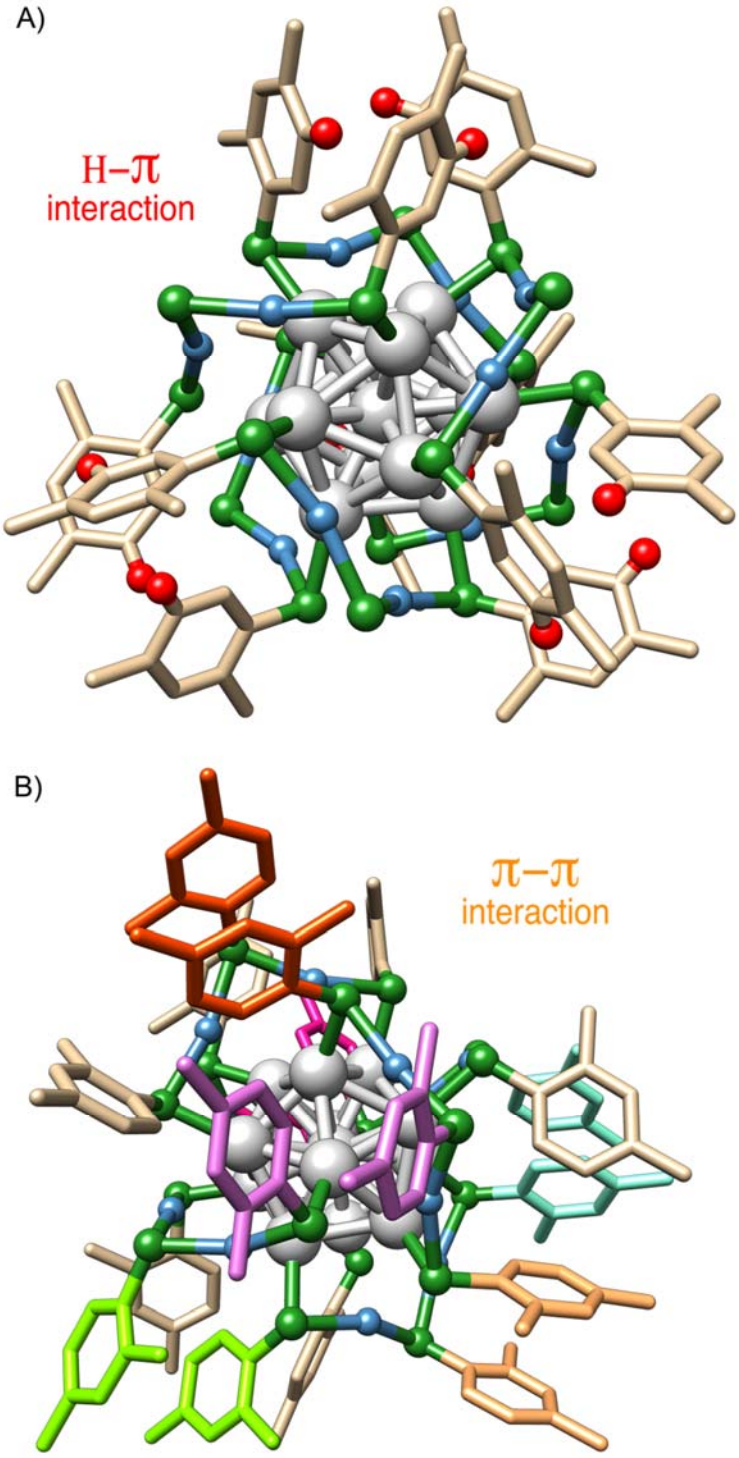

Figure S5: 3D representation of the X-ray structure of $[Ag_{25}(DMBT)_{18}]$ cluster.[1] A) Highlights of the four groups (one behind the silver core) of three DMPT ligands forming H-π interactions. B) Different colours are used to emphasize the six couples of DMBT ligands (one in "*in*" and one in "*out*" position) involved in the π-π interactions.

4. NMR characterization of $Ag_{25}(DMBT)_{18}$ in DMF-d_7

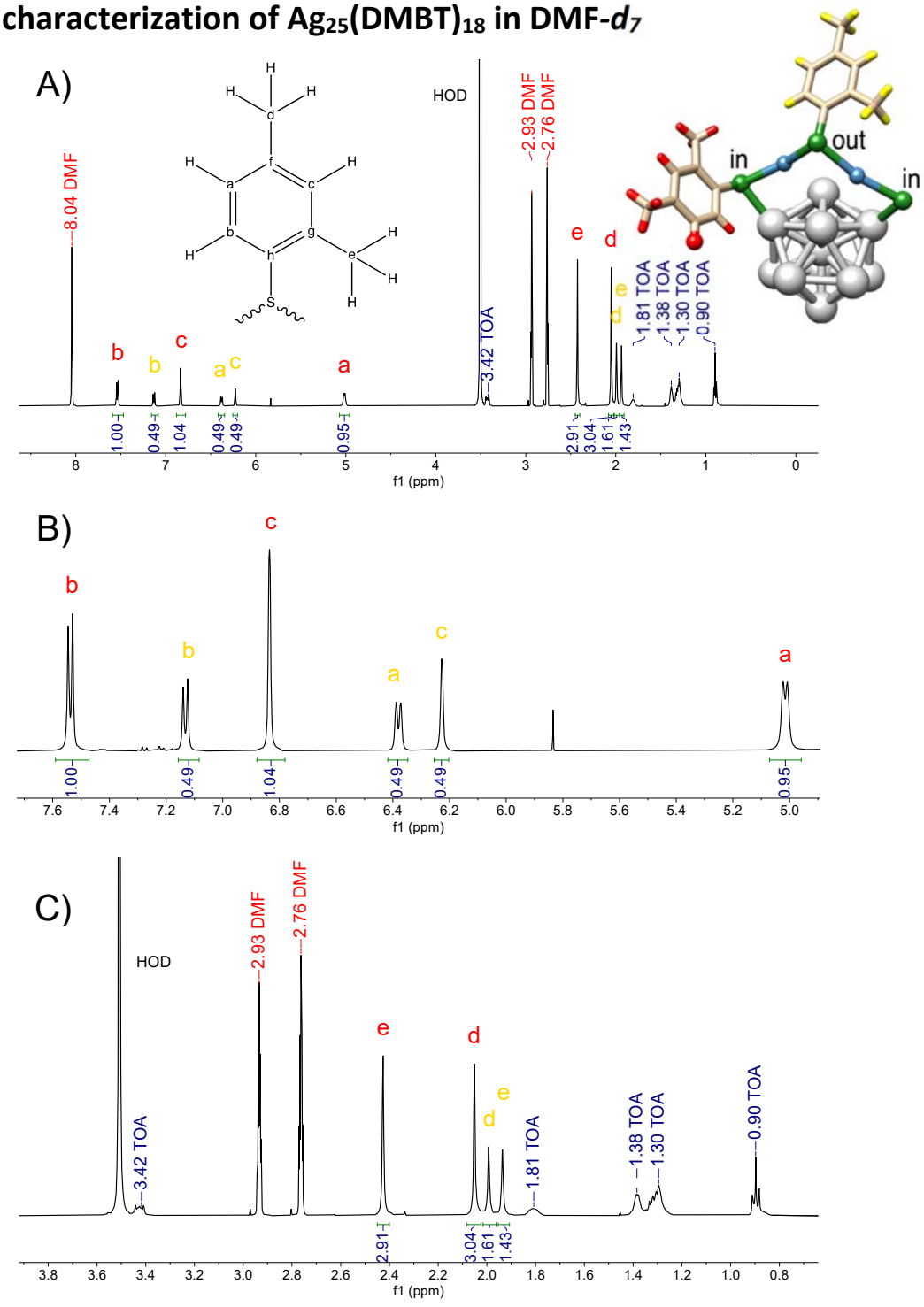

Figure S6: ^{1}H-NMR of [$Ag_{25}(DMBT)_{18}$] [TOA] cluster in DMF-d_7(*) at 298 K: A) entire spectra with relative integrals, B) aromatic region and C) aliphatic region. Red and yellow colors are employed to assign all the cluster's peaks to two symmetry-unique type of DMBT ligands, respectively "*out*" and "*in*" positions. Tetraoctylammonium counter ion (TOA^+) signals are also assigned. Ha_{out} (red) is the proton involved in the H-π interaction.

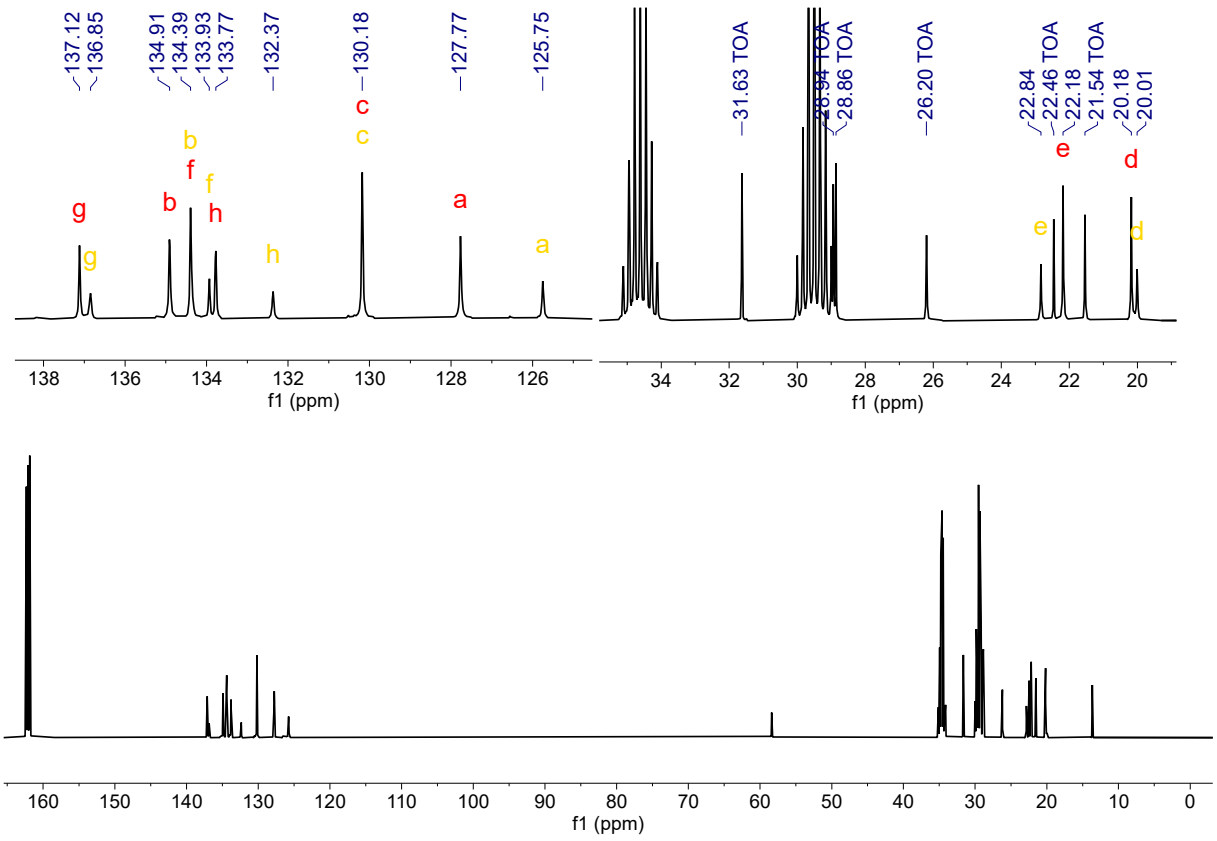

Figure S7: ^{13}C-NMR of $[Ag_{25}(DMBT)_{18}]$ [TOA] cluster in DMF-d_7 at 298 K. In the two insets are reported the aromatic and aliphatic region.

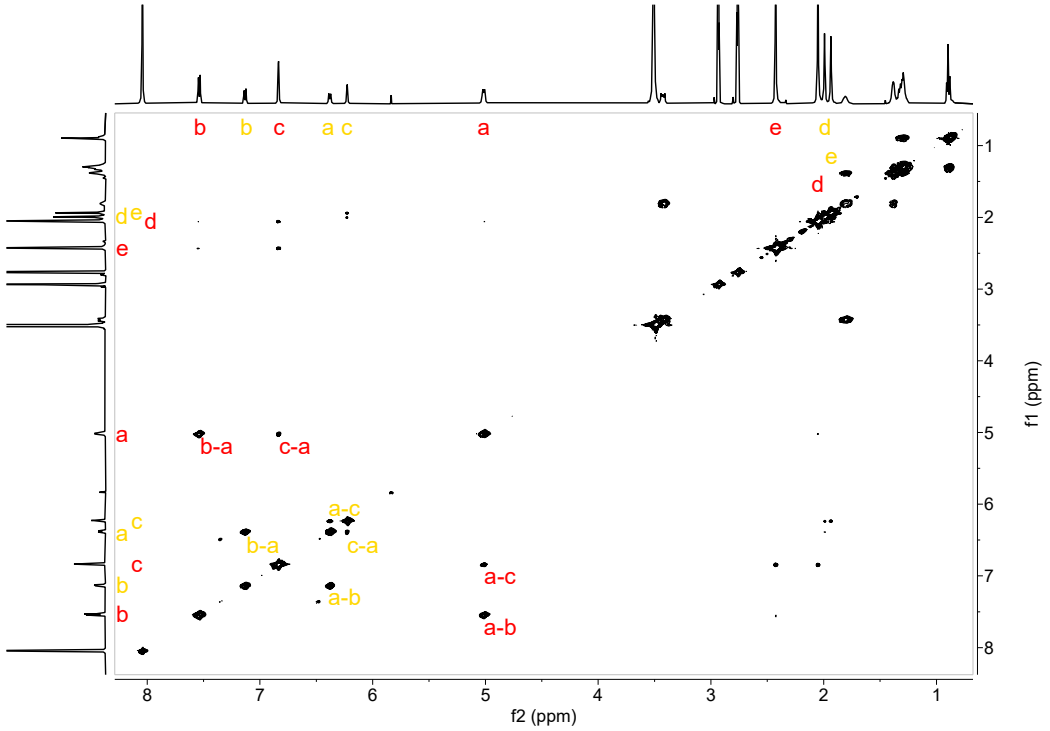

Figure S8: COSY spectra of $[Ag_{25}(DMBT)_{18}]$ [TOA] cluster in DMF-d_7 at 298 K

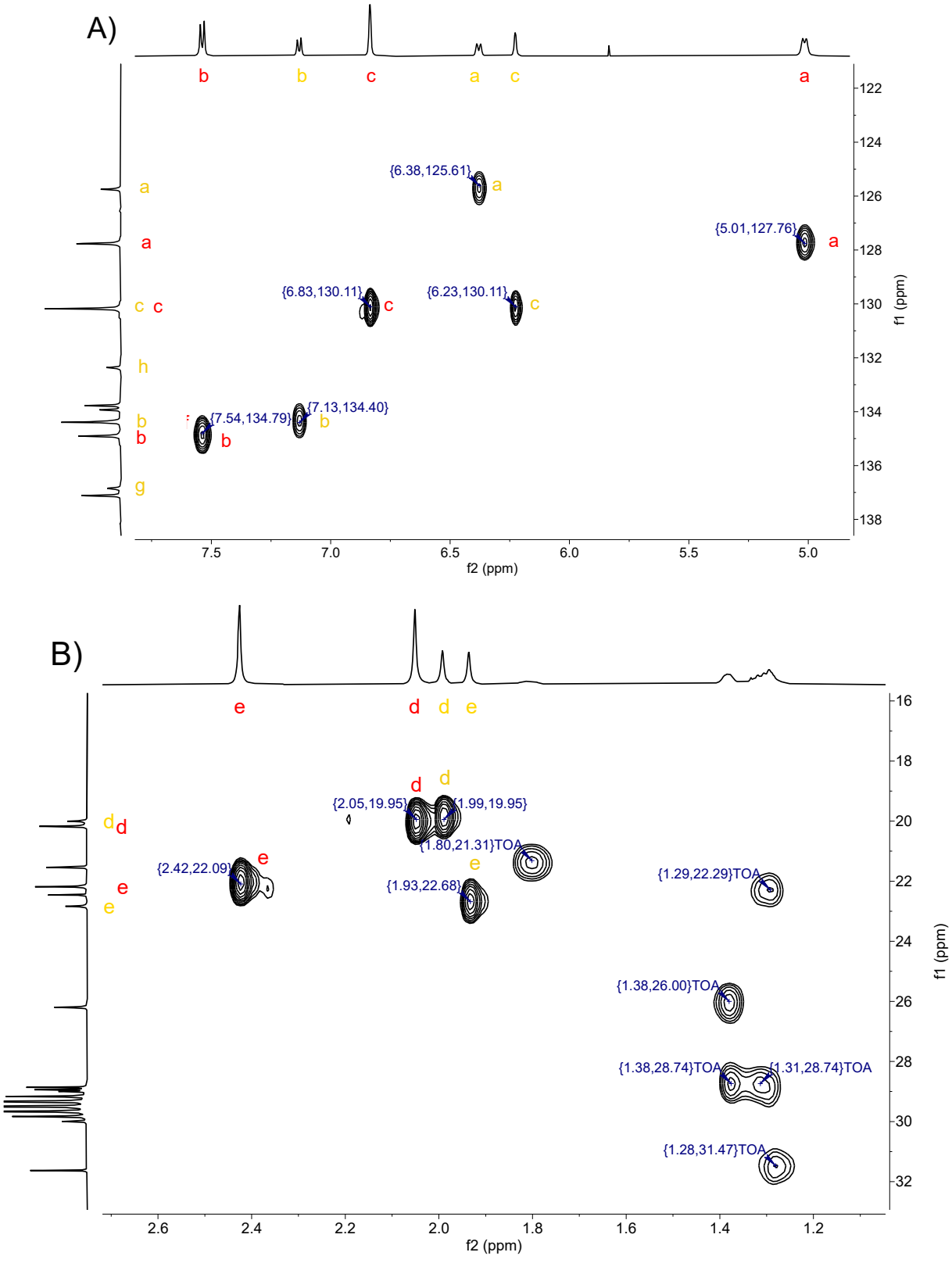

Figure S9: ^{1}H-^{13}C HSQC spectra of $[Ag_{25}(DMBT)_{18}]$ [TOA] cluster in DMF-d_7 at 298 K: A) aromatic region, B) aliphatic region.

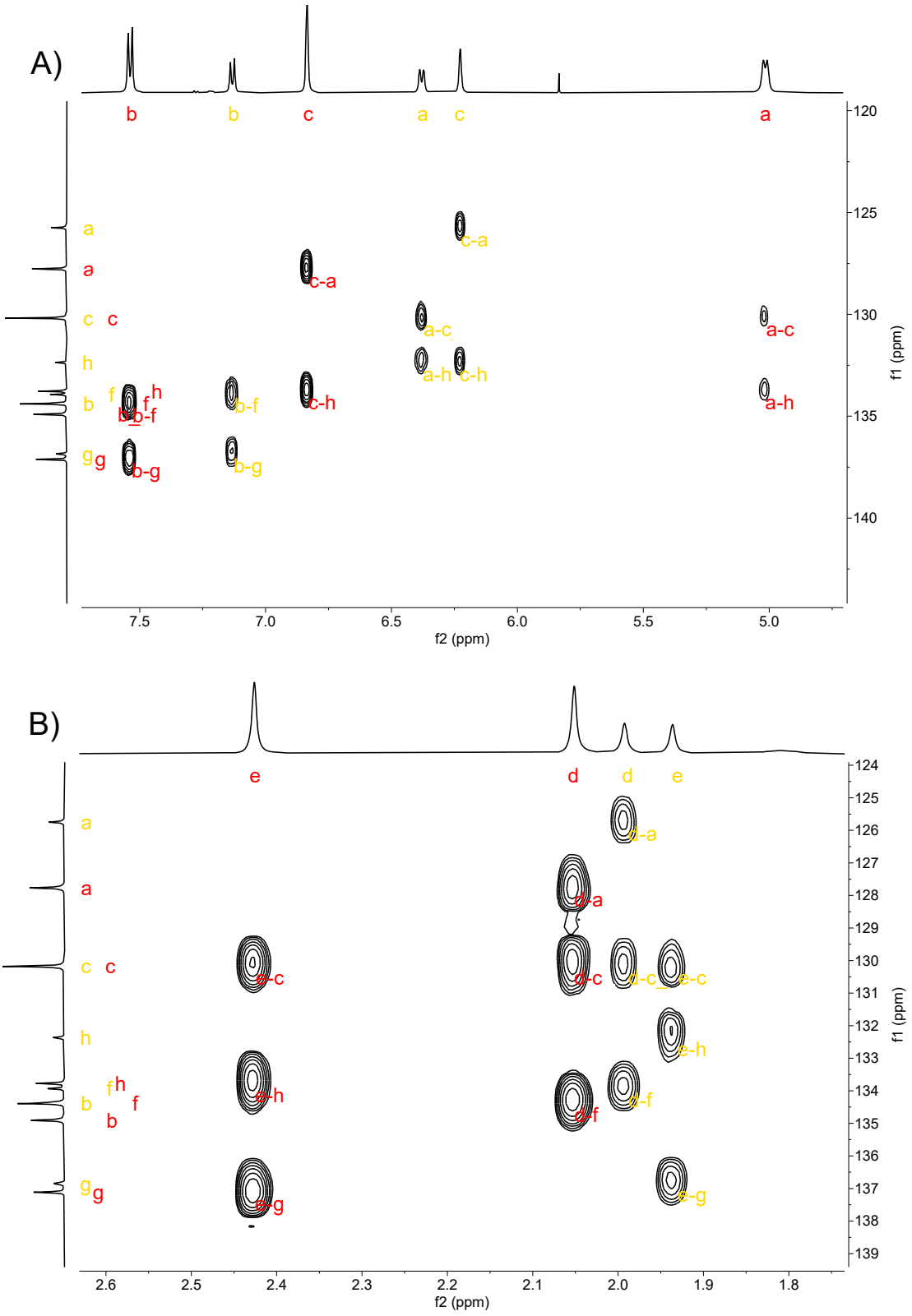

Figure S10: ^{1}H-^{13}C HMBC spectra of $[Ag_{25}(DMBT)_{18}]$ [TOA] cluster in DMF-d_7 at 298 K: A) aromatic protons region, B) aliphatic protons region.

5. Exchange Spectroscopy (EXSY)

The EXSY experiment is a powerful tool to determine rate constants and exchange pathways for exchange phenomenon. It is however important to note that the exchange rates which can be measured using this technique must correspond to the slow exchange regime ($k_{ex} \approx 10^{2}$-10^{-2} s^{-1}), so comparable to the longitudinal relaxation rates $k_{ex} \geq 1/T_1$. We refer the reader to the reviewer of Perrin and Dwyer[3] or Orrell [4] for examples of applications of 2D EXSY NMR.

Figure S11 shows a scheme of the EXSY experiment where initial ^{1}H transverse magnetization is generated through a radio-frequency (RF) fields for a $\pi/2$ pulse length. In the course of the evolution period (t_1) the magnetization vectors precess. The exchange process predominantly takes place during the mixing period, τ_m, while the magnetization is longitudinal and here τ_m ranged from 8 to 400 ms. The field gradient pulse destroys the remaining transverse components. The final $\pi/2$ pulse rotates the exchanged longitudinal magnetization into the xy plane for detection.

Here, we observe four distinct two-site proton exchange pathways between the *in* and *out* ligands of $[Ag_{25}(DMBT)_{18}][TOA]$. We do not observe a multisite exchange path as has been observed for a mixture of BCl_3 and BBr_3 for example.[5] Hence, the quantitative pseudo-first-order rate constant for two site exchange pathways were obtained by analyzing the experimental intensities of the NMR cross peaks obtained in EXSY experiments. This is achieved following the expressions derived by Macura and Ernst[6] for peak intensities as a function of rate constant *k*, mixing time τ_m and relaxation rate *R*. The theory underlying quantitative two-site exchange using ESXY experiments has been outlined in several articles.[3, 4, 7-9]

The determination of the proper mixing time is important for the successful application of EXSY in order to extract reliable numerical values of rate constants in addition to exchange pathway information. In practice the mixing time should be sufficient in magnitude to give relatively strong cross peaks but must not be so excessively long that the signal intensities become insensitive to the exchange rates. In absence of unknown rates, an upper limit can be defined from the knowledge that the rate constant at coalescence, k_c, is given by equation 1 where δ_ν is the different in Hz between the two exchanging sites in the slow exchange regime.[10] For the calculation we use the peak $Ha_{in}Ha_{out}$ which shows coalescence in the higher temperature NMR experiments.

$$k_c = \frac{\pi \delta_\nu}{\sqrt{2}} \text{ [1]}$$

Table S1. Table of first order exchange rate constants (s^{-1}) and approximation of the appropriate mixing time necessary for determination of quantitative rates constant for a two-site exchange measured by EXSY experiment.

Exchange cross peak	F2 (ppm)	F1 (ppm)	δ_ν (Hz)	k_c (s^{-1})	τ_m (ms)
$Ha_{in}Ha_{out}$	6.36	5.03	8	17.55	57

Figure S12 shows a graph of the intensities of cross peaks as a function of the mixing time, and this can also be used to determine the optimal mixing time as Abel et al. presented.[9] Signals have an optimum distribution of intensities and gradients when τ_m is approximately between 50 -75 ms. This is in agreement with the approximated value calculated with equation 1 of ~60 ms.

Error bars for the rate constants depend on the volume of the area of the cross peaks, and the noise of the spectrum.[11]

We also compare the experimental EXSY spectra to rotating- frame Overhauser enhancement spectroscopy (ROESY).[12, 13] This method is particularly suitable for heavy systems as such is ours (MW = 5166.7 Da), and have a motional correlation time τ_c near the condition of $\omega\ \tau_c = 1$, where ω is the Larmor frequency. In this case, the NOE is near zero but the ROE under spin lock is always positive in phase and increases with increasing value of τ_c. Figure S11 b shows the ROESY pulse sequence employed in this work where we see that a strong RF field is switched on (the spin lock) during the mixing period. During this exchange time, spin exchange among spin-locked magnetization components of different nuclei can occur. We are using a 180_x180_{-x} spin lock to remove the coherent magnetization transfer by TOCSY that occurs by *J*-coupling pathways.[13] It is normal that we also observe COSY-type cross peaks in a ROE spectrum when the spin lock can act analogous as a 90° pulse in a COSY experiment which allows coherence transfer between *J*-coupled spins.

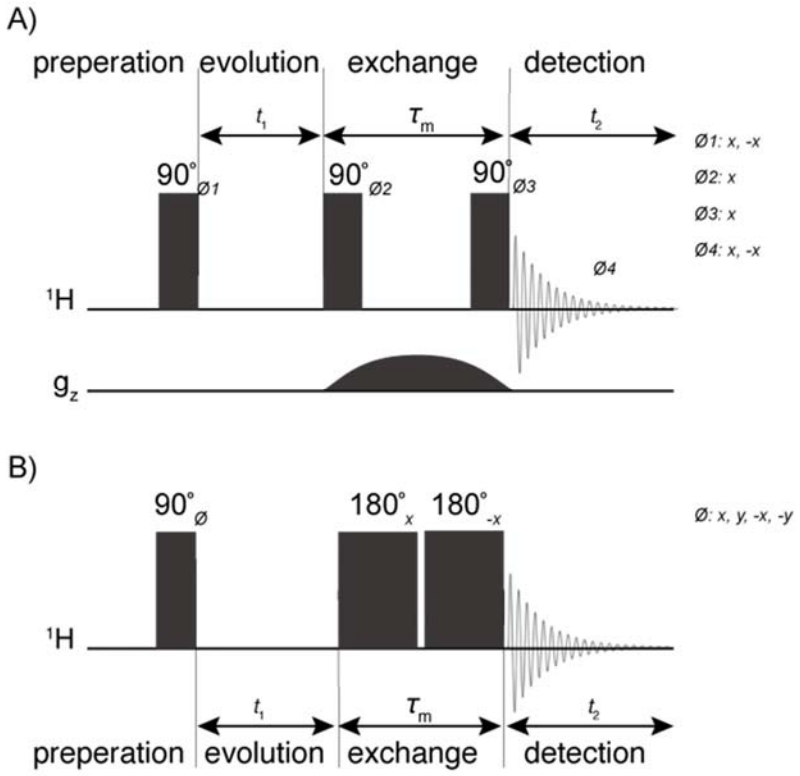

Figure S11. Basic pulse scheme of (a) phase sensitive exchange spectroscopy (EXSY) pulse sequence[14, 15] with gradient pulses during mixing time and (b) phase sensitive rotating frame overhauser effect spectroscopy (ROESY)[12, 13] with 180_x180_{-x} spinlock during mixing time used to study $[Ag_{25}(DMBT)_{18}][TOA]$.

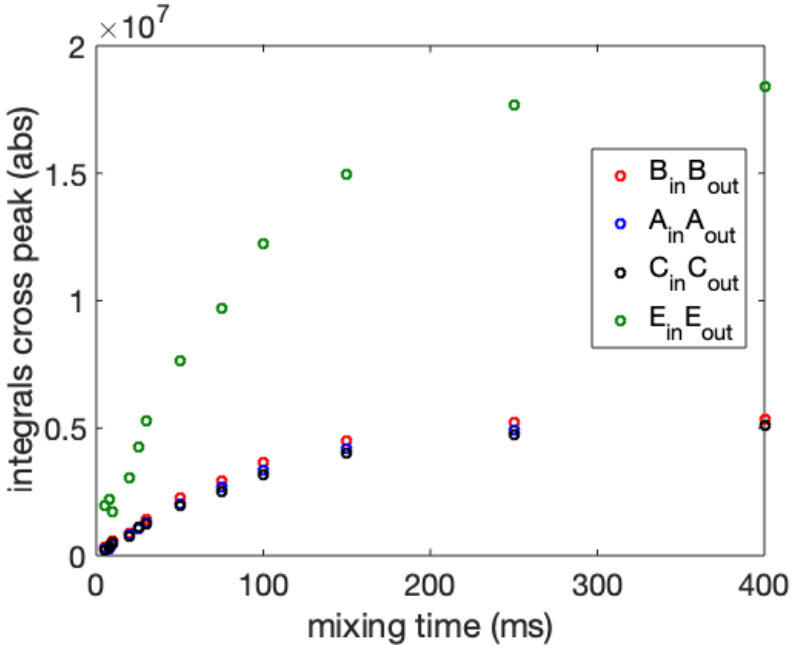

Figure S12. Plot of the mixing times as a function the integral of exchange cross peaks $Hb_{in}Hb_{out}$, $Ha_{in}Ha_{out}$, $Hc_{in}Hc_{out}$, $He_{in}He_{out}$ represent by red, blue, black and green circles.

Table S2. Values of pseudo-first order rate constants (s^{-1}) for two-site exchange of different protons between the chemically distinct *in* and *out* DMBT ligands of $[Ag_{25}(DMBT)_{18}][TOA]$ measured by EXSY experiment from the intensity of the exchange-cross peaks using a mixing period of 50 ms and measured at 298 K, and the reference EXSY experiment a mixing time of 5 ms.

Exchange cross peak	F2 (ppm)	F1 (ppm)	k'_a (s^{-1})	k'_b (s^{-1})
$Hc_{in}Hc_{out}$	6.82	6.23	2.089 ±0.014	4.564±0.032
$Hb_{in}Hb_{out}$	7.52	7.12	n.a.	n.a.
$Ha_{in}Ha_{out}$	6.36	5.03	2.028±0.011	3.996±0.023
$He_{in}He_{out}$	2.43	1.41	2.208±0.013	4.237±0.024

The factor of two between the forward, k'_a, and reverse, k'_b, pseudo-first order rate constants (s^{-1}) for the two proton-site exchange of the chemically distinct *in* and *out* DMBT ligands of $[Ag_{25}(DMBT)_{18}][TOA]$ confirms the relative population of 12 in-DMBT ligand to 6 out-DMBT ligands.[7, 11]

$$12\ in-DMBT\ \cdot k'_a = 6\ out-DMBT\ \cdot k'_b$$

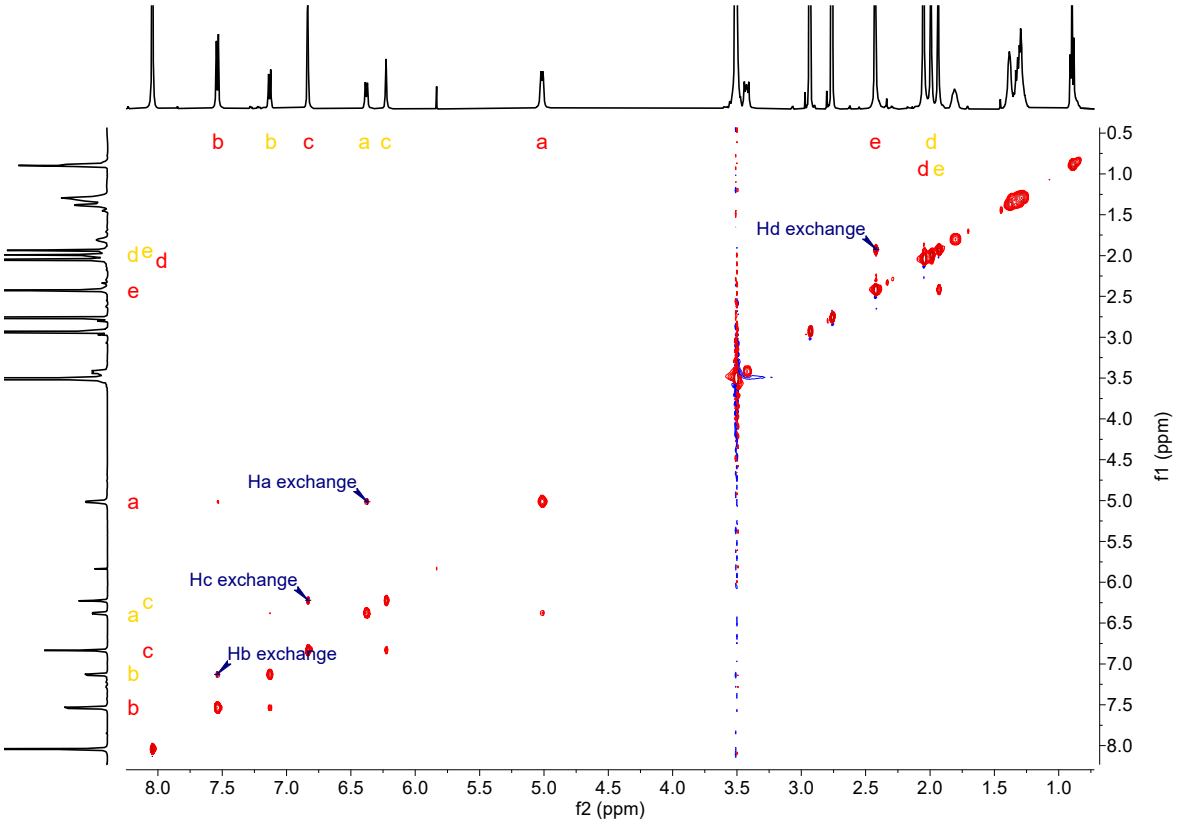

Figure S13. ^{1}H-^{1}H EXSY spectrum of $[Ag_{25}(DMBT)_{18}][TOA]$ acquired in DMF-d_7 at 298 K with a 50 ms mixing time.

6. NMR characterization of $AuAg_{24}(DMBT)_{18}$

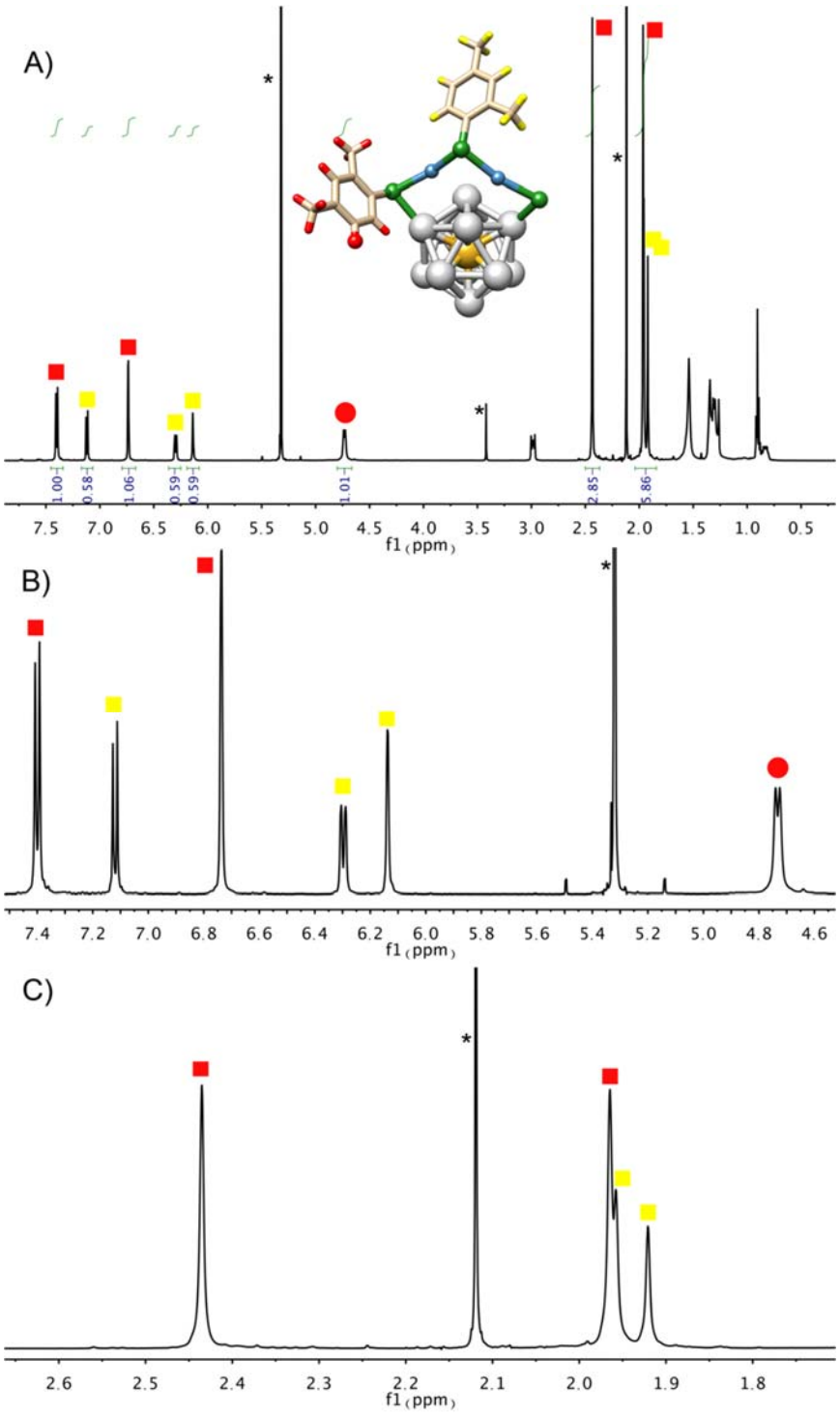

Figure S14: ^{1}H-NMR of [$AuAg_{24}(DMBT)_{18}$] [TOA] cluster in DCM-d_2 at 298 K: A) entire spectra with relative integrals, B) aromatic region and C) aliphatic region. Red and yellow squares are employed to assign all the cluster's peaks to two symmetry-unique type of DMBT ligands. The red circle is used to highlight the proton involved in the H-π interaction.

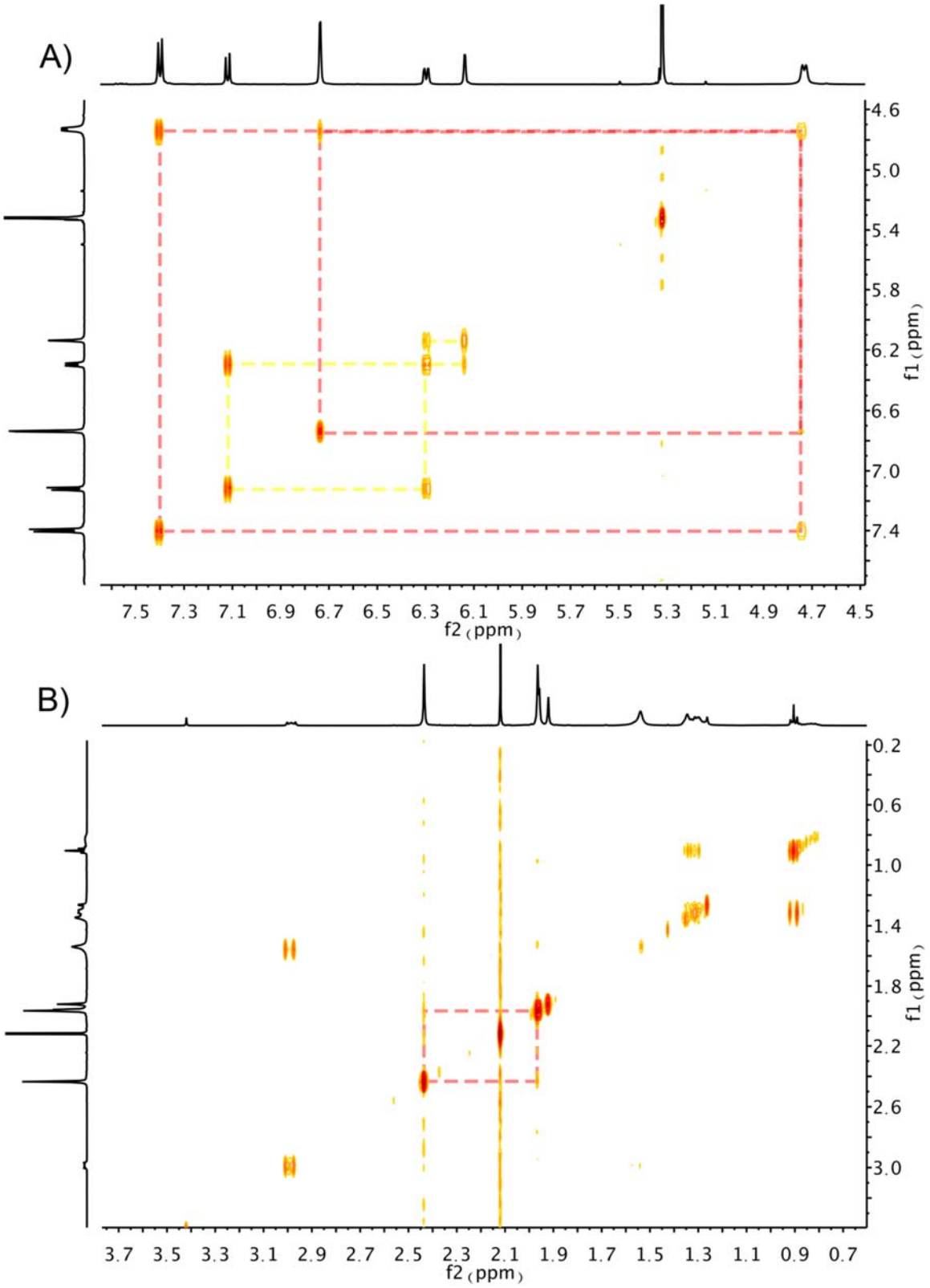

Figure S15: COSY spectra of $[AuAg_{24}(DMBT)_{18}]$ [TOA] cluster in DCM-d_2 at 298 K: A) aromatic region, B) aliphatic region. Red and yellow squares are employed to assign all the cross-peaks relative to two symmetry-unique type of DMBT ligands.

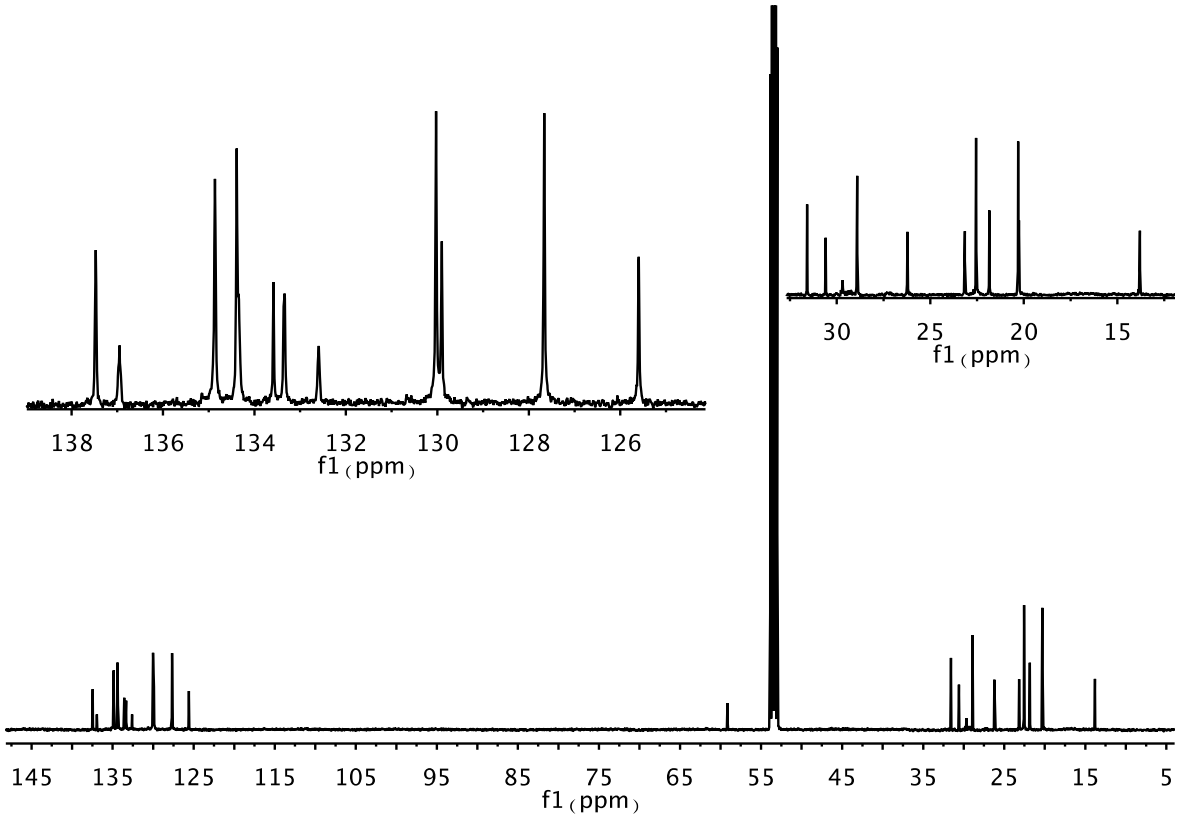

Figure S16: ^{13}C-NMR of [$AuAg_{24}(DMBT)_{18}$] [TOA] cluster in DCM-d_2 at 298 K. In the two insets are reported the aromatic and aliphatic region.

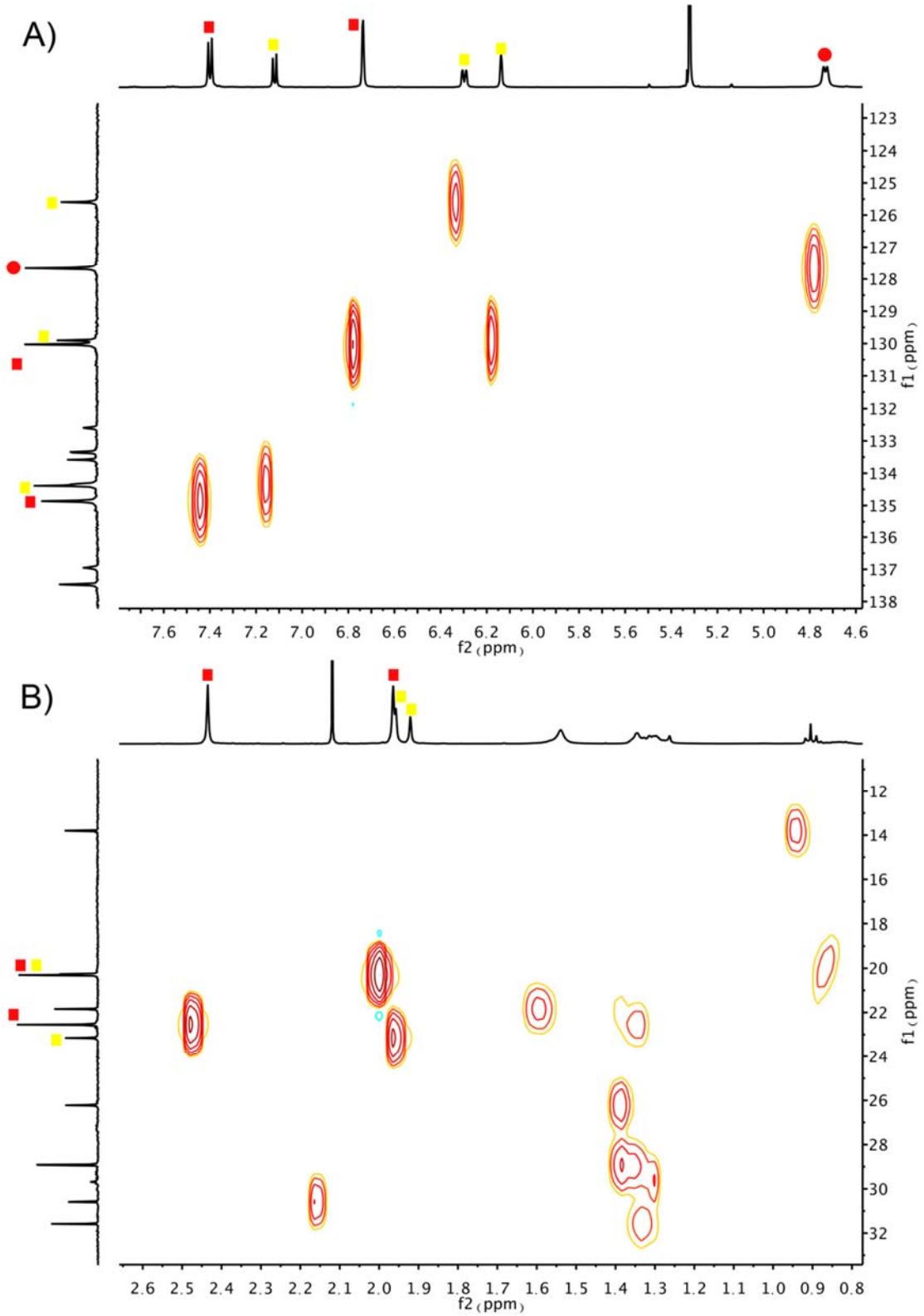

Figure S17: ^{1}H-^{13}C HSQC spectra of $[AuAg_{24}(DMBT)_{18}]$ [TOA] cluster in DCM-d_2 at 298 K: A) aromatic region, B) aliphatic region. Red and yellow squares are employed to assign all the cluster's peaks to two symmetry-unique type of DMBT ligands.

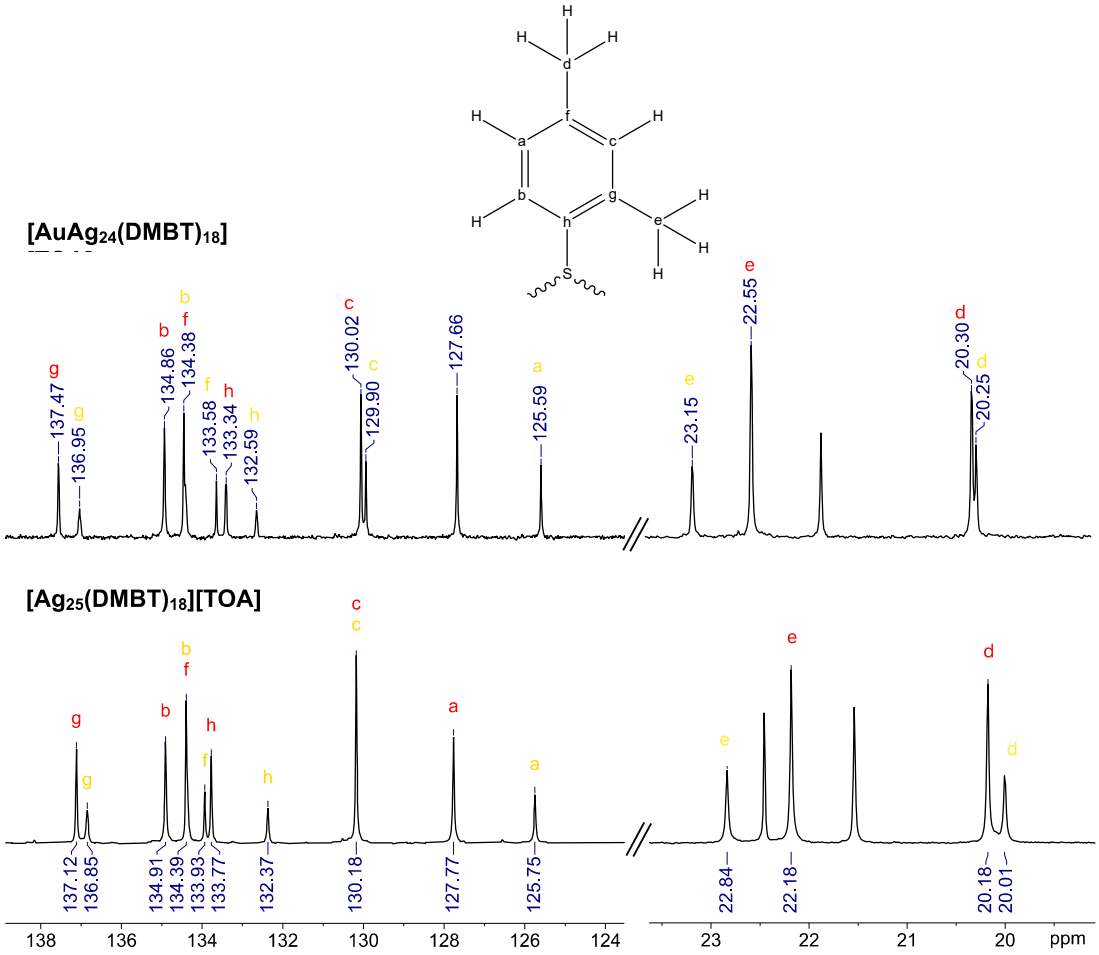

Figure S18: Overlaid ^{13}C NMR spectra of the aromatic (left) and aliphatic (right) region of $[AuAg_{24}(DMBT)_{18}]$ [TOA] cluster (top), $[Ag_{25}(DMBT)_{18}]$ [TOA] cluster (bottom) in DCM-d_2 at 298 K. Assignment of the chemically inequivalent ligands follows the scheme in the inset, and chemical shifts are shown in directly on the spectra.

Figure S18 shows the ^{13}C NMR spectra of the aromatic (left) and aliphatic (right) region of $[AuAg_{24}(DMBT)_{18}]$ [TOA] cluster (top), $[Ag_{25}(DMBT)_{18}]$ [TOA] cluster (bottom) in DCM-d_2 at 298 K. We do observe the expected chemical shift change for the quaternary C_h, in closest contact with the surface of the NC. The $\delta_{iso}(^{13}C_h)$ of DMBT out ligand of Ag_{25} NC is more shielded ($\delta_{iso}(^{13}C_h)$= 132.37 ppm) with respect to the $AuAg_{24}$ ($\delta_{iso}(^{13}C_h)$= 132.59 ppm). This trend is also observed for the Me C_e for both *in* and *out* DMBT ligands.

This is the opposite trend that was previously established in sodium citrate capped Au nanoparticles, where the carboxylate carbon interacting directly with the surface is more shielded (($\delta_{iso}(^{13}C)$= 162, 164 or 167 ppm for ligand Au NPs versus the 181 ppm crystalline ligand).[16] The shift of a few ppm and opposite trend for the NCs as compared to the NPs, can be rationalized by the fact that in the NCs there is an atom of sulfur between the C atom and the surface of $AuAg_{24}$ (and also there is only one Au atom for twenty four Ag).

7. Variable temperature NMR experiments

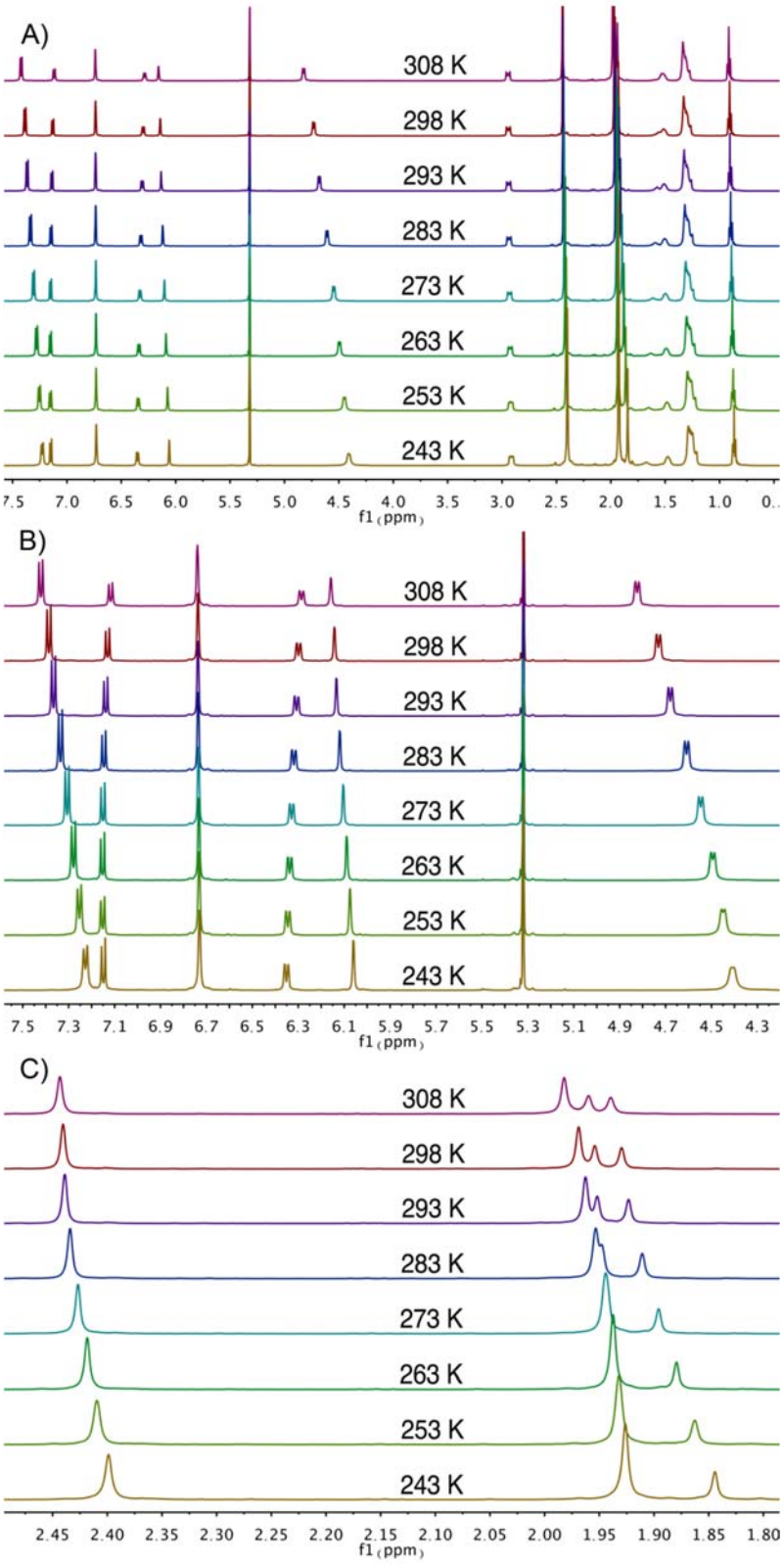

Figure S19: ^{1}H-NMR spectra of $[Ag_{25}(DMBT)_{18}]$ [TOA] cluster in DCM-d_2 at different temperatures (243 K - 308 K): A) entire spectra, B) aromatic region and C) aliphatic region.

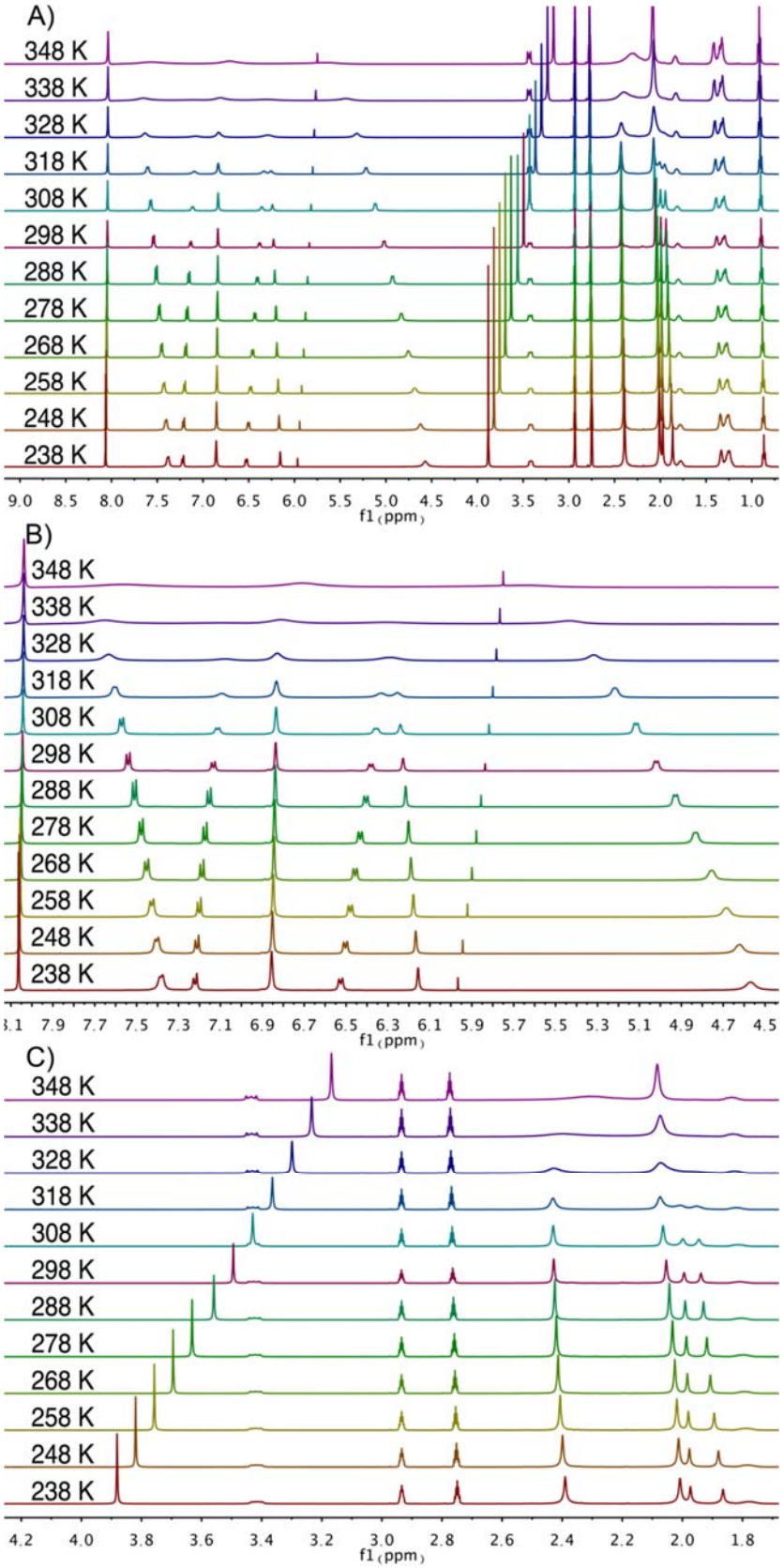

Figure S20: ^{1}H-NMR spectra of $[Ag_{25}(DMBT)_{18}]$ [TOA] cluster in DMF-d_7 at different temperatures (238 K - 348 K): A) entire spectra, B) aromatic region and C) aliphatic region.

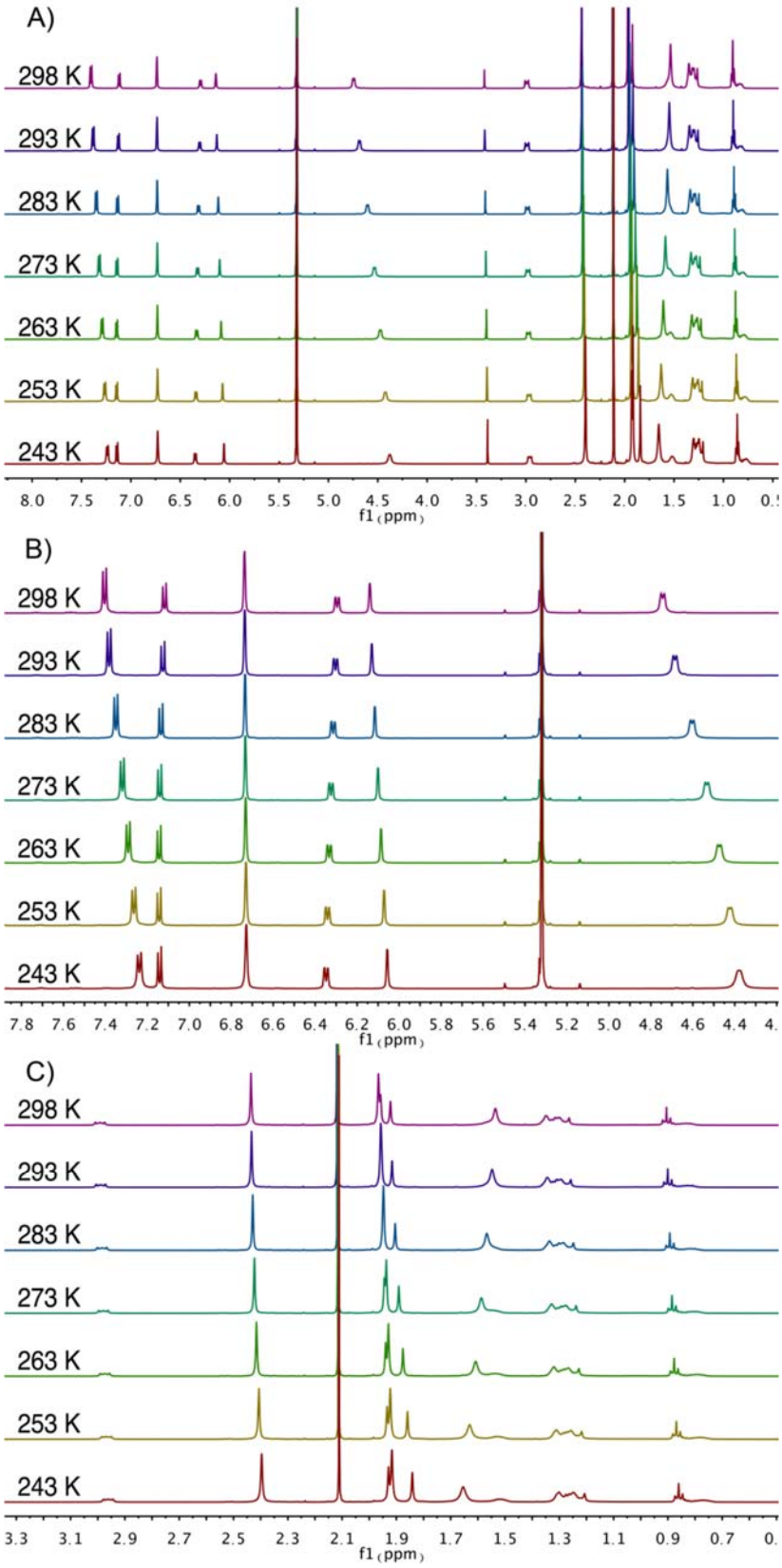

Figure S21: ^{1}H-NMR spectra of [$AuAg_{24}(DMBT)_{18}$] [TOA] cluster in DCM-d_2 at different temperatures (238 K - 348 K): A) entire spectra, B) aromatic region and C) aliphatic region.

8. NMR titration experiments

NMR titrations with hexafluorobenzene (HFB). 1-30 μL aliquots of pure HFB were added stepwise to 0.6 mL of a solution of $[Ag_{25}(DMBT)_{18}]$ [TOA] in DCM-d_2 with a concentration in DMBT thiols of 2.9×10^{-2} M (concentration of cluster 1.6×10^{-3} M) in screwcap NMR tube. After each addition a ^{1}H-NMR and a ^{19}F-NMR spectra were acquired.

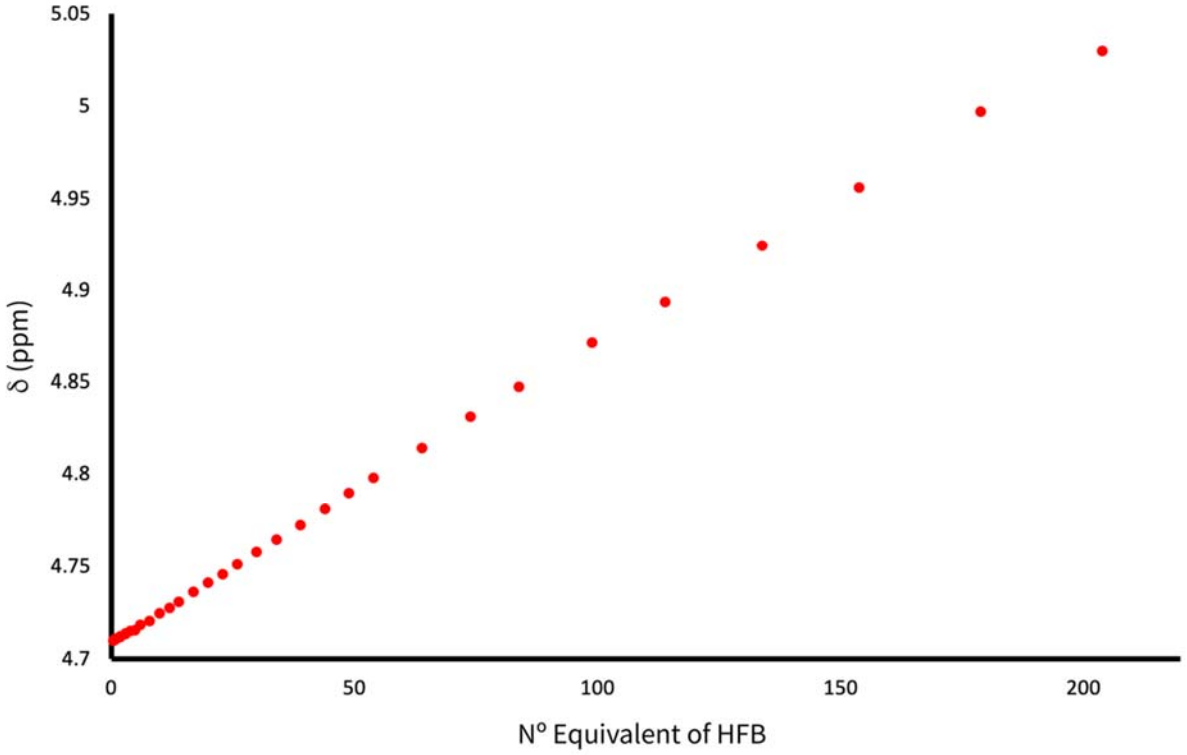

Figure S22: ^{1}H-NMR titration of $[Ag_{25}(DMBT)_{18}]$ [TOA] cluster with HFB (up to 204 equivalent) in DCM-d_2 at 298 K. On the X axis is reported the numbers of equivalents of HFB and on the Y axis the variation of chemical shift of the proton involved in the H-π interaction.

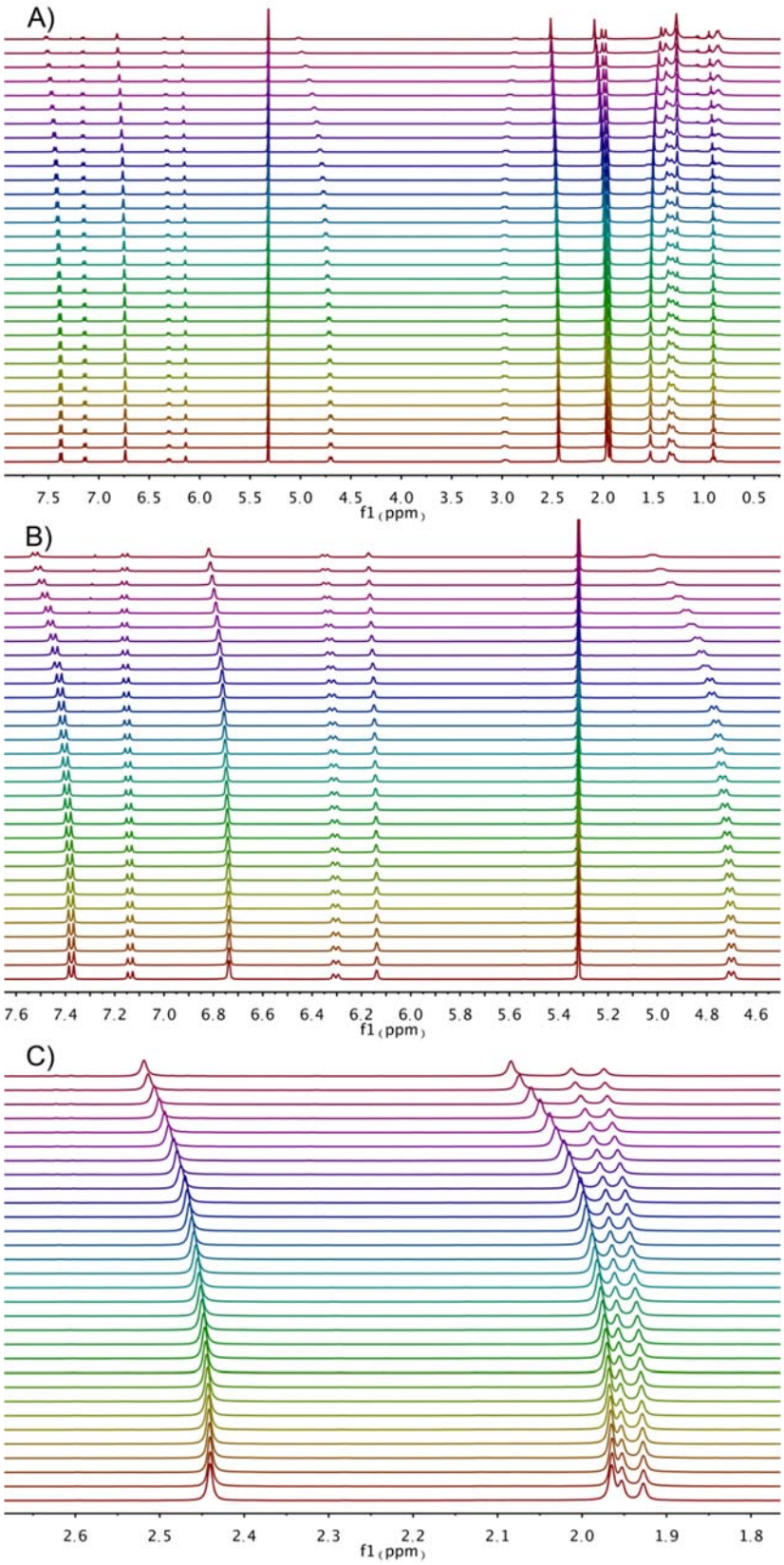

Figure S23: ^{1}H-NMR titration of $[Ag_{25}(DMBT)_{18}]$ [TOA] cluster with HFB (up to 204 equivalent) in DCM-d_2 at 298 K: A) entire spectra with relative integrals, B) aromatic region and C) aliphatic region.

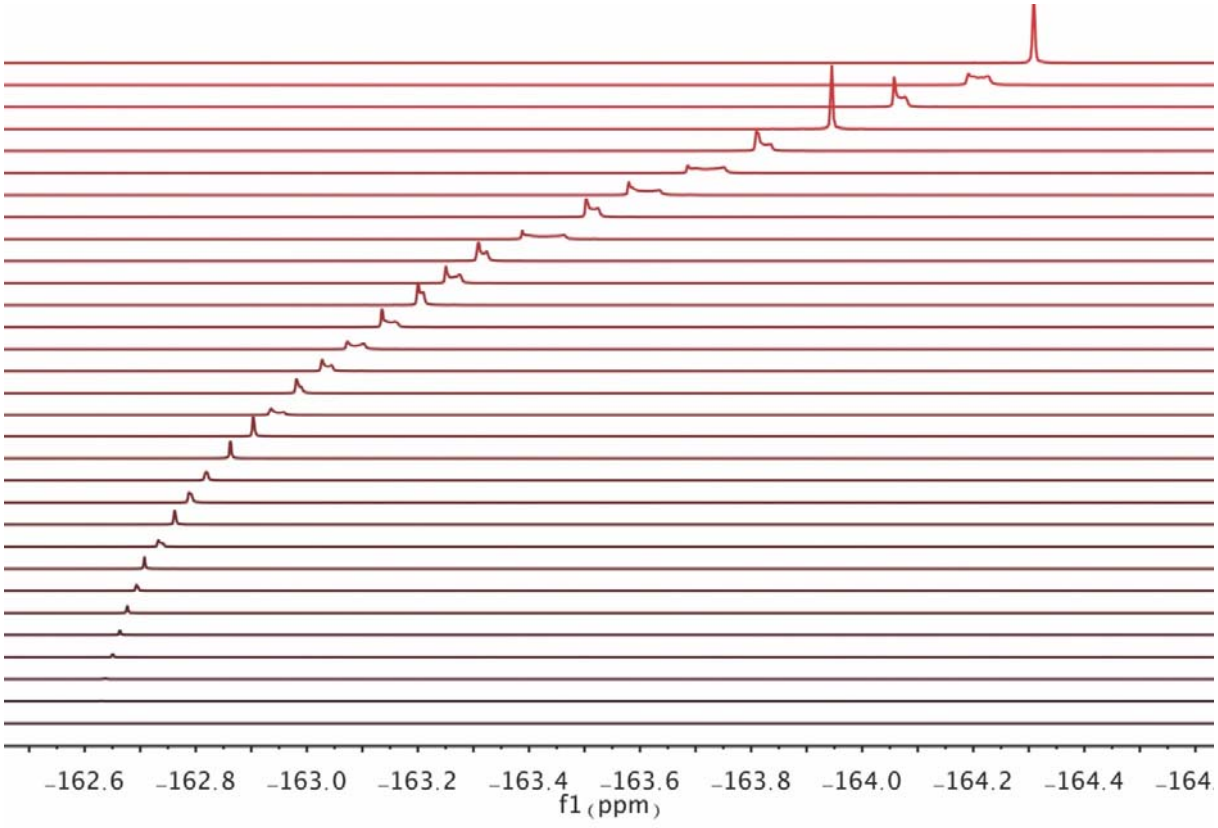

Figure S24: ^{19}F-NMR titration of $[Ag_{25}(DMBT)_{18}]$ [TOA] cluster with HFB in DCM-d_2 at 298 K.

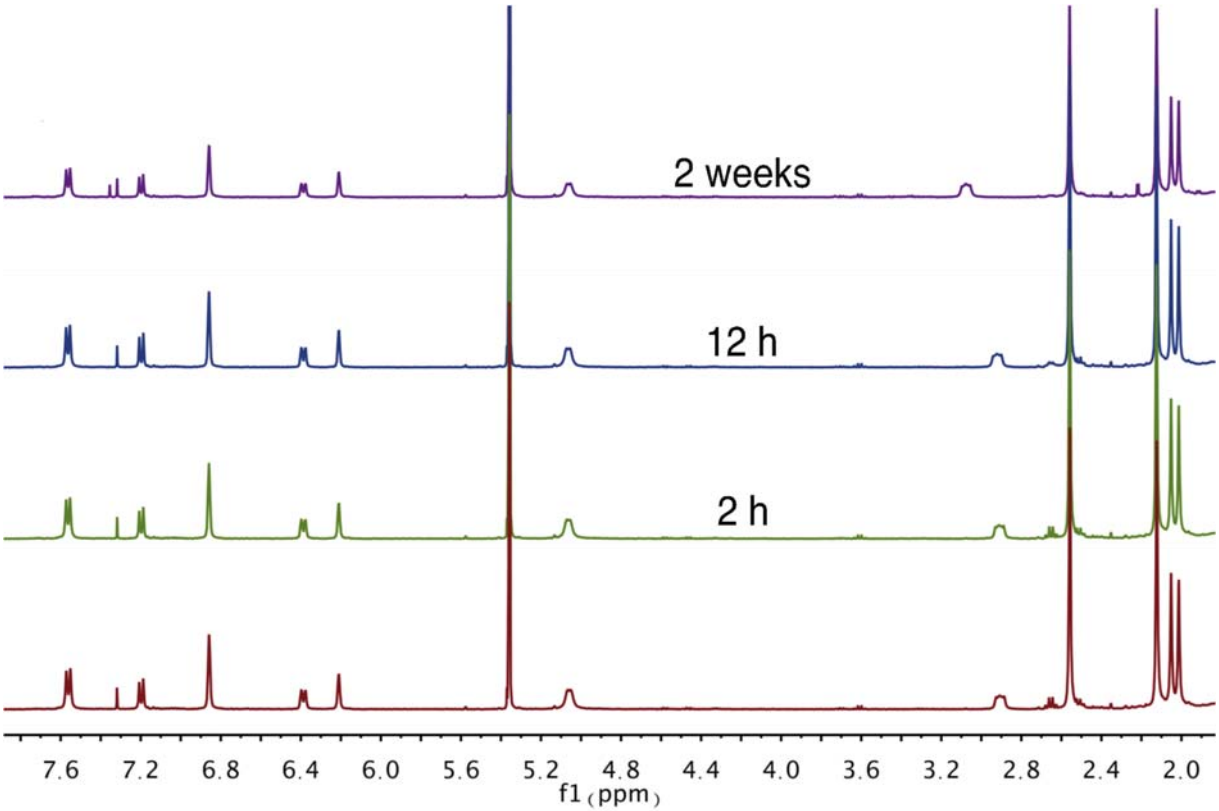

Figure S25: ^{1}H-NMR spectra of $[Ag_{24}(DMBT)_{18}]$ [TOA] cluster with 204 equivalents of HFB in DCM-d_2 at 298 K after: 2 hours, 12 hours and 2 weeks. The minimum decomposition of the cluster was observed after 2 weeks as highlighted by the minimum difference between the intensity of signals in the different spectra.

9. NMR experiments in toluene

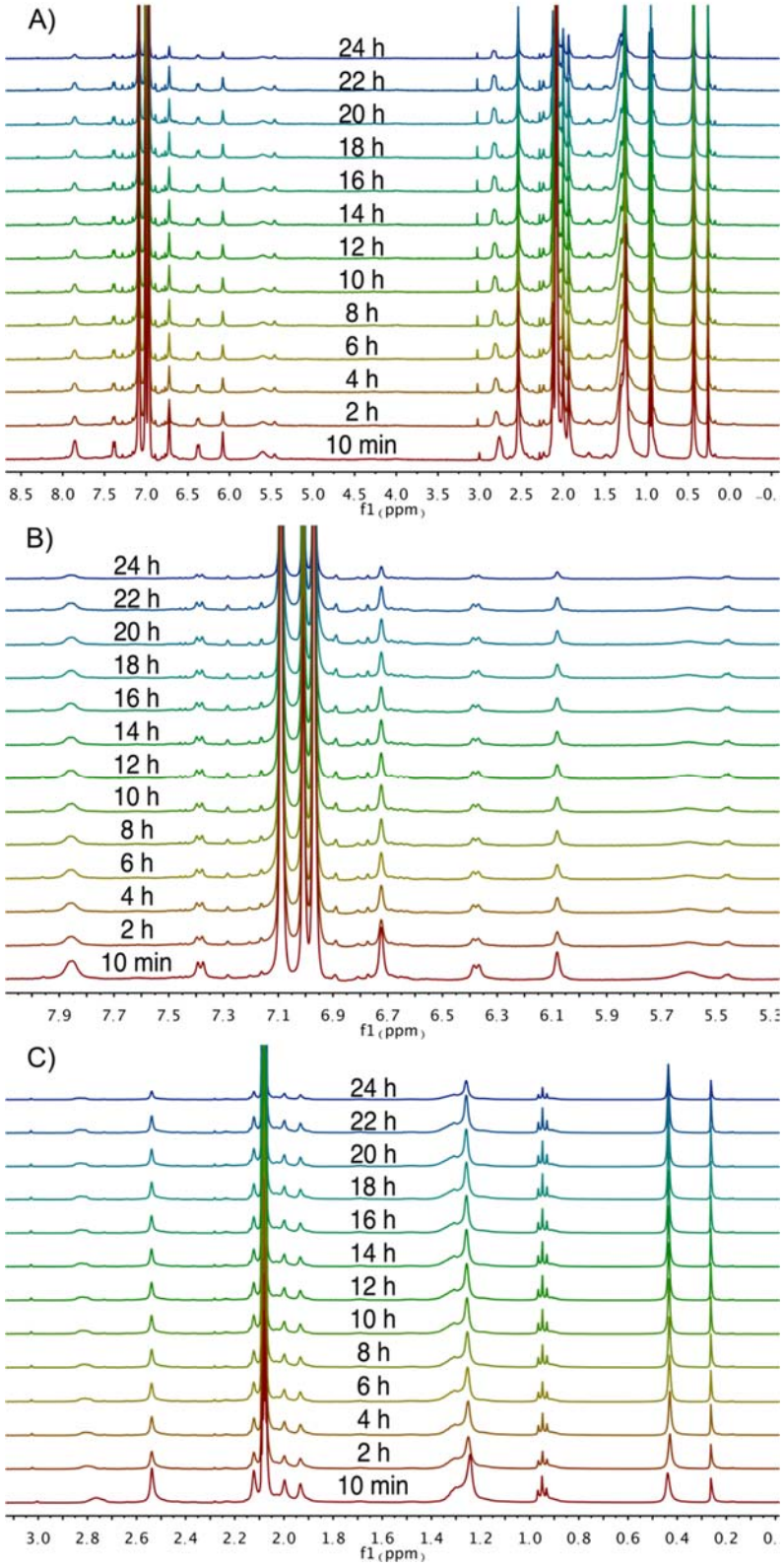

Figure S26: ^{1}H-NMR spectra of $[Ag_{25}(DMBT)_{18}]$ [TOA] cluster in Tolune-$d_8$over 24 hours: A) entire spectra, B) aromatic region and C) aliphatic region.

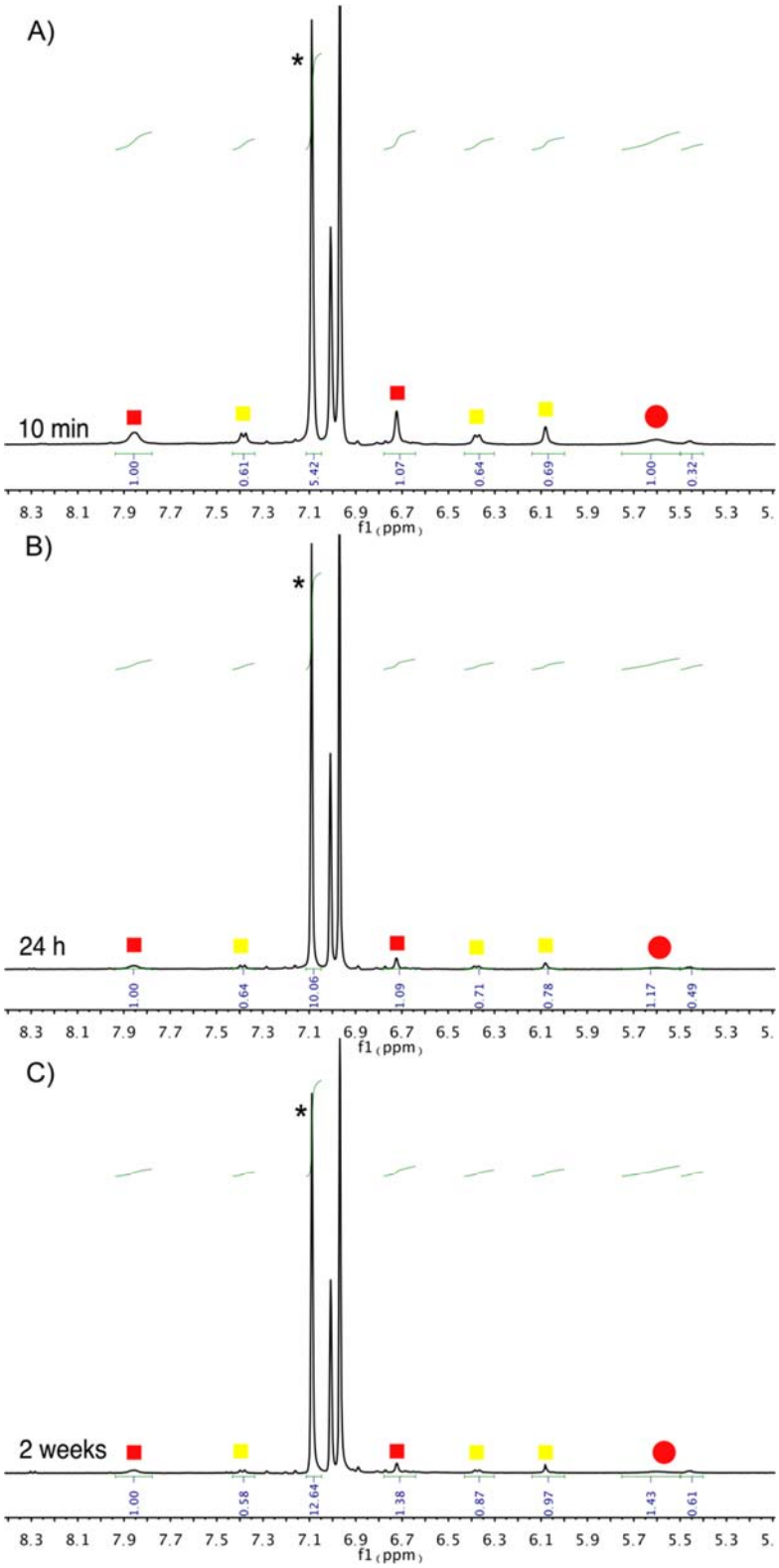

Figure S27: ^{1}H-NMR spectra (aromatic region) of $[Ag_{25}(DMBT)_{18}]$ [TOA] cluster in Tolune-$d_8$after: A) 10 minutes, B) 24 hours and C) 2 weeks. The decomposition of the cluster is highlighted by the increasing difference between the integrals of its protons in comparison with the integral of toluene (*, used as internal standard).

10. References

1. Joshi, C. P.; Bootharaju, M. S.; Alhilaly, M. J.; Bakr, O. M., [Ag 25 (SR) 18] − : The " Golden " Silver Nanoparticle. *J. Am. Chem. Soc.* **2015,** *137*, 11578-11581.
2. Bootharaju, M. S.; Joshi, C. P.; Parida, M. R.; Mohammed, O. F.; Bakr, O. M., Templated atom-precise galvanic synthesis and structure elucidation of a [Ag24Au(SR)18]- nanocluster. *Angew. Chem. Int. Ed.* **2016,** *55* (3), 922-926.
3. Perrin, C. L.; Dwyer, T. J., Application of Two-Dimmensional NMR to Kinetics of Chemical Exchange. *Chemical Review* **1990,** *90*, 935-967.
4. Orrell, K. G., Two-Dimensional Methods of Monitoring Exchange. In *Encyclopedia of Magnetic Resonance*, 2007.
5. Derose, E. f.; Castillo, J.; Saulys, D.; Morrison, J., A Two-Dimensional Boron-11 NMR study of Halogen Scrambling in a Mixture of BCl3 and BBr3. *J. Magn. Reson.* **1991,** *93*, 347-354.
6. Macura, S.; Ernst, R. R., Elucidation of Cross Relaxation in Liquids by Two-Dimensional NMR Spectroscopy. *Mol. Phys.* **1980,** *41*, 95-117.
7. Reseach, M., EXSY CALC: NMR analysis of molecular systems undergoing chemical exchange. *Mestrelab Application Note* **2007,** .
8. Zolnai, Z.; Juranic, N.; Vikic-Topic, D.; Macura, S., Quantitative Determination of Magnetization Exchange Rate Constants from a Series of Two-Dimensional Exchange NMR Spectra. *J. Chem. Inf. Comput. Sci.* **2000,** *40*, 611-621.
9. Abel, E. W.; Coston, T. J.; Orrel, K. G.; Sik, V.; Stephenson, D., Two-Dimensional NMR Exchange Spectroscopy. Quantitative Treatment of Multisite Exchange Systems. *J. Magn. Reson.* **1986,** *70*, 34-53.
10. Claridge, T. D. W., Chapter 8: Correlations through space. In *High-Resolution NMR Techniques in Organic Chemistry*, Bäckvall, J. E.; Baldwin, J. E.; Williams, R. M., Eds. Tetrahedron Organic Chemistry Series: 2009; Vol. 27, pp 247-301.
11. Perrin, C. L.; Dwyer, T. J., Application of Two-Dimensional NMR to Kinetics of Chemical Exchange. *Chem. Rev.* **1990,** *90* (6), 935-967.
12. Bax, A.; Davis, D. G., Practical Aspects of Two-Dimensional Transverse NOE Spectroscopy. *J. Magn. Reson.* **1985,** *63*, 207-213.
13. Hwang, T. L.; Shaka, A.-J., Cross Relaxation without TOCSY: Transverse Rotating-Frame Overhausser Effect Spectroscopy. *J. Am. Chem. Soc.* **1992,** *114*, 3157-3159.
14. Jeener, J.; Meier, B. H.; Bachmann, P.; Ernst, R. R., Investigation of exchange processes by two-dimensional NMR spectroscopy. *J. Chem. Phys.* **1979,** *71* (11), 4546-4553.
15. Wagner, R.; Berger, S., Gradient-Selected NOESY- A fourfold Reduction of the Measurement Time for the NOESY Experiment. *J. Magn. Reson.* **1996,** *123*, 119-121.
16. Al-Johani, H.; Abou-Hamad, E.; Jedidi, A.; Widdifield, C. M.; Viger-Gravel, J.; Sangaru, S. S.; Gajan, D.; Anjum, D. H.; Ould-Chikh, S.; Hedhili, M. N.; Gurinov, A.; Kelly, M. J.; El Eter, M.; Cavallo, L.; Emsley, L.; Basset, J.-M., The structure and binding mode of citrate in the stabilization of gold nanoparticles. *Nat. Chem.* **2017,** *9* (9), 890-895.